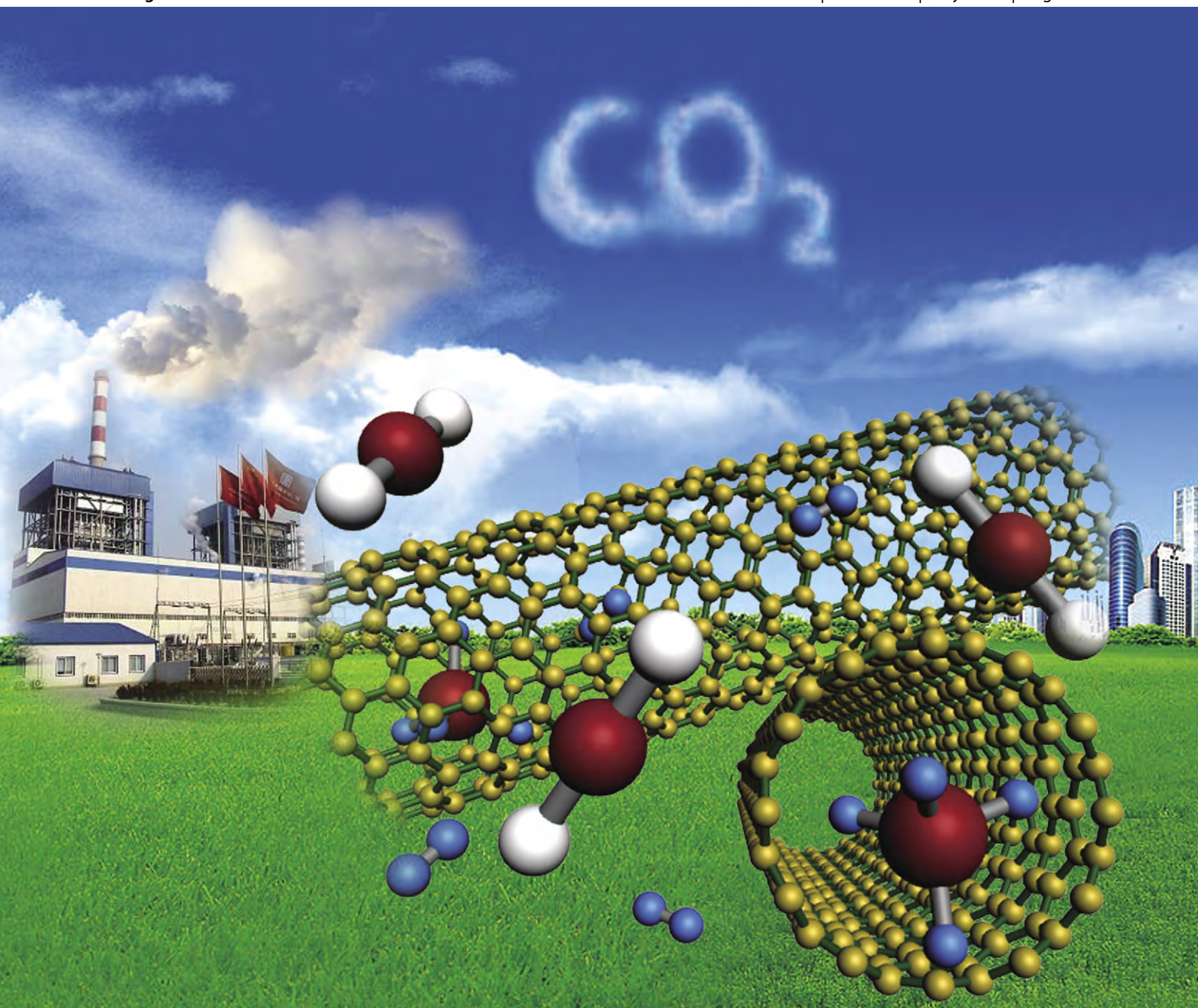


Chem Soc Rev

Chemical Society Reviews

www.rsc.org/chemsocrev

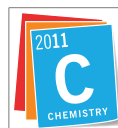
Volume 40 | Number 7 | July 2011 | Pages 3369–4260



ISSN 0306-0012

RSC Publishing

CRITICAL REVIEW
Wei Wang, Shengping Wang,
Xinbin Ma and Jinlong Gong
Recent advances in catalytic
hydrogenation of carbon dioxide



International Year of
CHEMISTRY
2011



0306-0012(2011)40:7;1-U

Cite this: *Chem. Soc. Rev.*, 2011, **40**, 3703–3727

www.rsc.org/csr

Recent advances in catalytic hydrogenation of carbon dioxide

Wei Wang, Shengping Wang, Xinbin Ma and Jinlong Gong*

Received 9th January 2011

DOI: 10.1039/c1cs15008a

Owing to the increasing emissions of carbon dioxide (CO₂), human life and the ecological environment have been affected by global warming and climate changes. To mitigate the concentration of CO₂ in the atmosphere various strategies have been implemented such as separation, storage, and utilization of CO₂. Although it has been explored for many years, hydrogenation reaction, an important representative among chemical conversions of CO₂, offers challenging opportunities for sustainable development in energy and the environment. Indeed, the hydrogenation of CO₂ not only reduces the increasing CO₂ buildup but also produces fuels and chemicals. In this *critical review* we discuss recent developments in this area, with emphases on catalytic reactivity, reactor innovation, and reaction mechanism. We also provide an overview regarding the challenges and opportunities for future research in the field (319 references).

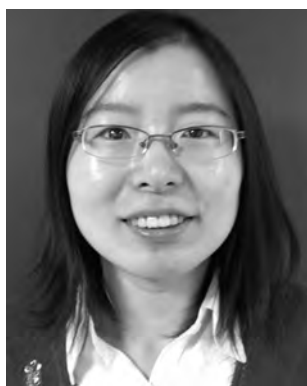
1. Introduction

For the past centuries, utilization of carbon-rich fossil fuels—coal, oil, and natural gas—has allowed an unprecedented era of prosperity and advancement for human development.¹ However, the concentration of carbon dioxide in the atmosphere has consequently risen from ~280 ppm before the industrial revolution to ~390 ppm in 2010, which is further predicted to be ~570 ppm by the end of the century.² The increase in CO₂ emissions arguably contributes to the increase in global temperatures and climate changes due to the “greenhouse effect”. Hence, there has been increasing pressure for countries and scientists to curb CO₂ emissions and develop efficient CO₂ capture and utilization systems.^{3,4}

Reducing CO₂ emissions is an extensive and long-term task. In principle, there are three possible strategies with this regard—reduction of the amount of CO₂ produced, storage of CO₂, and usage of CO₂.^{2,5,6} The first strategy requires energy efficient improvements and switching from fossil fuels toward less carbon intensive energy sources such as hydrogen and renewable energy.⁵ Storage of CO₂, involving the development of new technologies for capture and sequestration of CO₂, is a relatively well established process.^{2,5,7,8}

As an economical, safe, and renewable carbon source, CO₂ turns out to be an attractive C₁ building block for making organic chemicals, materials, and carbohydrates (*e.g.*, foods).⁹ The utilization of CO₂ as a feedstock for producing chemicals not only contributes to alleviating global climate changes caused by the increasing CO₂ emissions, but also provides a grand challenge in exploring new concepts and opportunities for catalytic and industrial development.¹⁰ However, CO₂ is

Key Laboratory for Green Chemical Technology of Ministry of Education, School of Chemical Engineering and Technology, Tianjin University, Tianjin 300072, China. E-mail: jlgong@tju.edu.cn



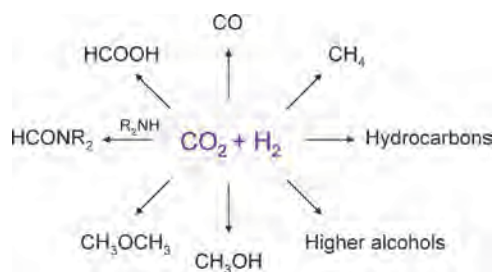
Wei Wang

Wei Wang obtained her BS (2005) and MS (2007) degrees in chemical engineering from Tianjin University. After one year stay in the Key Laboratory for Green Chemical Technology of MoE as a research assistant, she started her PhD course in 2008 under the supervision of Professors Xinbin Ma and Jinlong Gong. Wang is interested in designing and synthesizing novel metal oxides for chemical conversion of carbon dioxide.



Shengping Wang

Shengping Wang earned her BS (1994) and MS (2000) degrees from Hebei University of Technology and her PhD degree (2003) from Tianjin University, all in Chemical Engineering. She has been an associate professor of Tianjin University since 2005. She has interests in capture and conversion of carbon dioxide, and synthesis of organic carbonates.



Scheme 1 Products from CO₂ hydrogenation covered in this review.

not used extensively as a source of carbon in current laboratory and industrial practices. Indeed, the use of CO₂ as chemical feedstock is limited to a few industrial processes—synthesis of urea and its derivatives, salicylic acid, and carbonates. This is primarily due to the thermodynamic stability of CO₂ and thus high energy substances or electroreductive processes are typically required to transform CO₂ into other chemicals.^{11–13}

Hydrogen is a high energy material and can be used for CO₂ transformation as the reagent. The main products of CO₂ hydrogenation can fall into two categories—fuels and chemicals (Scheme 1). Indeed, the needs for fuels are ever-increasing with growing energy consumption. However, the resources of fossil fuels are being diminished and fuel prices have undergone strong fluctuation in recent years. Therefore, it would be highly desirable to develop alternative fuels from non-fossil fuel sources and processes. The products of CO₂ hydrogenation such as methanol, dimethyl ether (DME), and hydrocarbons, are excellent fuels in internal combustion engines, and also are easy for storage and transportation. Furthermore, methanol and formic acid are raw materials and intermediates for many chemical industries. However, we must

recall potential issues associated with hydrogen such as production, storage, and transportation. Hydrogen sources for the chemical recycling of CO₂ could be generated either by using still-existing significant sources of fossil fuels (mainly natural gas) or from splitting water (by electrolysis or other cleavage).¹

Hydrogenation of CO₂ has been more intensively investigated recently, due to fundamental and practical significance in the context of catalysis, surface science, biology, nanoscience and nanotechnology, and environmental science. Both homogeneous and heterogeneous catalysts have been used to hydrogenate CO₂.^{10,14,15} Homogeneous catalysts show satisfactory activity and selectivity, but the recovery and regeneration are problematic. Alternatively, heterogeneous catalysts are preferable in terms of stability, separation, handling, and reuse, as well as reactor design, which reflects in lower costs for large-scale productions.^{6,11,12,14,16,17} To combine the desirable reactivity of homogeneous catalysts with the recyclability of heterogeneous catalysts, significant progress has been made in this direction, including the immobilization of homogeneous catalysts, exploitation of novel heterogeneous catalysts, and the use of green solvents such as ionic liquids (ILs) and supercritical CO₂ (scCO₂).^{18–20}

There have been several excellent reviews regarding CO₂ conversions as well as catalytic hydrogenation of CO₂.^{3,6,9,11,14–16,21–28} However, these reviews primarily focus on general aspects of CO₂ applications and homogeneously catalyzed hydrogenation of CO₂.^{15,29–31} Advances have been made in the past decade, especially on hydrogenation of CO₂ *via* heterogeneous catalysts. Therefore, this critical review attempts to provide current understanding of catalytic reactivity, reactor innovation, and reaction mechanism over various types of catalysts, particularly over heterogeneous catalysts with an emphasis on practical aspects.



Xinbin Ma

Xinbin Ma received BS and MS degrees in Chemical Engineering from Tianjin University. He obtained his PhD degree in Chemical Engineering from Tianjin University in 1996 under the tutelage of Hongfang Chen and Genhui Xu. He continued his academic career as an assistant professor in the same department, and was promoted to full professor in 2004. His main scientific interests are conversion of C₁ molecules and synthesis of organic carbonates and oxalates.



Jinlong Gong

Jinlong Gong studied chemical engineering and received his BS and MS degrees from Tianjin University and his PhD degree from the University of Texas at Austin under the guidance of C. B. Mullins. He was a visiting scientist at the Pacific Northwest National Laboratory in 2007. After a stint with Professor George M. Whitesides as a postdoctoral research fellow at Harvard University, he joined the faculty of Tianjin University, where he is currently a full professor in chemical engineering. He is the recipient of numerous awards including a Chinese Government Award for Outstanding Graduate Students Abroad, an International Precious Metals Institute Research Award, and an IUPAC Prize for Young Chemists-Honorable Mention Award. His research interests in surface science and catalysis include catalytic conversions of green energy, novel utilizations of carbon dioxide, and synthesis and applications of nanostructured materials.

2. Synthesis of carbon monoxide *via* reverse water gas shift (RWGS) reaction

Catalytic conversion of CO₂ to CO *via* RWGS reaction has been generally deemed as one of the most promising processes for CO₂ conversions.³²



Indeed, the RWGS reaction occurs in many processes, wherever CO₂ and H₂ are present in a reaction mixture. Due to the importance of this reaction from both fundamental and practical points of view, the design and characterization of RWGS catalysts have attracted considerable attention.

2.1 Metal-based heterogeneous catalysts

As RWGS is a reversible reaction, catalysts active in the water gas shift (WGS) reaction are often active in the reverse reaction.¹⁶ Copper-based catalysts, the most popularly studied catalytic systems for the WGS reaction, have also been applied to the RWGS reaction. Liu *et al.* have developed a series of bimetallic Cu–Ni/ γ -Al₂O₃ catalysts for CO₂ hydrogenation.³³ The ratio of Cu/Ni has a significant effect on conversion and selectivity. Cu favors CO formation, while Ni is active for CH₄ production. Cu/ZnO and Cu–Zn/Al₂O₃ catalysts used for methanol synthesis and WGS reaction have also been tested for the RWGS reaction.³⁴ The most active catalyst for the reaction is Cu rich (Cu/Zn > 3) with alumina as a support. A linear relationship between the activity of the catalyst and the surface area of metallic Cu was obtained.³⁴ Additionally, Chen *et al.* have reported that Cu/SiO₂ with a potassium promoter offers better catalytic activity (12.8% of CO₂ conversion at 600 °C) than that without promoter (5.3% of CO₂ conversion at 600 °C).³⁵ The created new active sites located at the interface between copper and potassium favor the formation of formate (HCOO) species, which is the key intermediate for CO production. The major role of K₂O is to provide active sites for decomposition of formates, in addition to acting as a promoter for CO₂ adsorption.

RWGS reaction is an endothermic reaction, and thus high temperature would facilitate the formation of CO. However, copper-based catalyst is not suitable at high temperature because of its poor thermal stability (*e.g.*, sintering of copper nanoparticles) unless modified by adding a thermal stabilizer. For example, upon the addition of a small amount of iron, catalytic activity and stability of Cu/SiO₂ at high temperature can be effectively improved.^{36,37} Large copper surface area is provided by Cu–Fe catalysts, even if the catalysts are pretreated at high temperature. At 600 °C and atmospheric pressure, the Cu–Fe catalysts exhibit high and stable catalytic activity up for 120 h. In contrast, 10 wt% Cu/SiO₂ without Fe additives deactivates rapidly, due to the decreased surface area of copper and oxidation of copper at high temperature.³⁷ The new active species around the interface between Cu and Fe particles were proposed to account for the enhanced catalytic activity. At high temperature, the sintering of Cu is effectively prevented by the formation of small particles of iron species around Cu particles.³⁷ Chen *et al.* have developed a Cu/SiO₂ catalyst by atomic layer epitaxy (ALE), which have favorable thermal stability to resist the sintering of Cu particles under

high temperature condition.³⁸ Due to the formation of small Cu particles, the ALE–Cu/SiO₂ catalysts could strongly bind CO and provide high catalytic activity for the RWGS reaction.

Cerium-based catalysts are also active in both WGS and RWGS reactions.³⁹ Ni/CeO₂ (2 wt% Ni) showed excellent catalytic performance in terms of activity, selectivity, and stability for the RWGS reaction.⁴⁰ CO yield is ~35% at 600 °C for a continuous period of 9 h. Oxygen vacancies formed in the lattice of ceria and highly dispersed Ni are key active components for the reaction, and bulk Ni favors the formation of methane. However, deactivation of ceria-supported catalysts is a crucial issue we need to consider. It has been reported that a very small coverage of deposited carbon on the ceria support leads to strong deactivation of the catalyst, indicating that the fraction of the support involved in the reaction is small, probably located next to the supported metal.⁴¹

Supported noble metal catalysts (*e.g.*, Pt, Ru, and Rh) typically have high ability toward H₂ dissociation, and thus they have been used as efficient catalysts for CO₂ hydrogenation. Bando *et al.* performed CO₂ hydrogenation over Li-promoted Rh ion-exchanged zeolites (Li/RhY).⁴² Main product transforms from methane to CO with increased amount of Li. When an atomic ratio of Li/Rh is higher than 10, the main product becomes CO (87% of selectivity) and formation of methane is greatly suppressed (8.4% of selectivity). The presence of Li atoms on the surface creates new active sites that enhance CO₂ adsorption and stabilization of adsorbed CO species.⁴²

Moreover, the type of metal precursor employed in the catalyst preparation affects catalytic reactivity. Arakawa *et al.* prepared silica-supported Rh catalysts (Rh/SiO₂) from acetate, chloride, and nitrate precursors *via* impregnation for CO₂ hydrogenation.⁴³ The main product was CO over the catalysts prepared from acetate and nitrate, whereas the amount of CH₄ was relatively high using the catalyst synthesized from the chloride precursor. Detailed X-ray photoelectron spectroscopy (XPS) measurements elucidated the effect of metal precursor on the CO₂ hydrogenation reactivity. It was found that the ratio of hydroxyl species to Rh atoms on SiO₂ surface determined reactivity (high ratio favors the formation of CO). The ratio based on different metal precursors follows the order: chloride < nitrate < acetate.⁴³

2.2 Reactor aspects

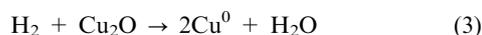
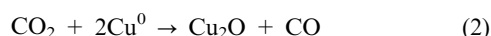
It has been generally recognized that the fluidized beds can be utilized efficiently for multiphase reactions such as the catalytic hydrogenation of CO₂, because it can achieve higher mass and heat transfer rates in comparison with any other contacting mode.⁴⁴ For instance, a fluidized bed reactor was used to investigate the characteristics of the RWGS reaction with Fe/Cu/K/Al catalyst; CO₂ conversion in the fluidized bed reactor (46.8%) was higher than that in the fixed bed reactor (32.3%).⁴⁵

Electrochemical promotion of the RWGS reaction has been studied in the solid oxide fuel cell (SOFC). For Cu/SrZr_{0.9}Y_{0.1}O_{3– α} , higher reaction rates were observed when hydrogen was electrochemically supplied as H⁺ than as

molecular hydrogen.⁴⁶ In case of Pt/YSZ (yttrium-stabilized zirconia), the rate-determining step of the RWGS reaction is the formation of surface-bound carbon and its interaction with adsorbed hydrogen.⁴⁷ The observation is due to the combination of direct electrocatalysis (electrodecomposition of CO₂, electro-oxidation of H₂) and electrochemical promotion. For Pd/YSZ, CO formation is improved by up to 6 times upon employing either negative or positive overpotentials.⁴⁸ SOFC displays great stability and durability in the RWGS reaction, and can be considered as one of the alternative routes for the production of renewable energy.

2.3 Reaction mechanism

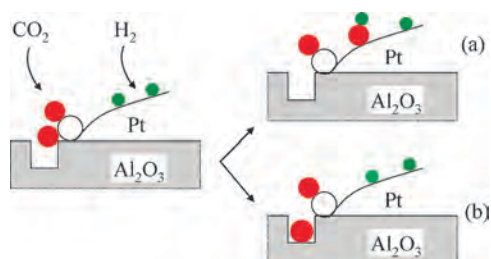
Considerable work has been recently conducted with a variety of advanced characterization tools to unravel mechanism of the RWGS reaction. The mechanism of the reaction has been primarily discussed over Cu-based catalysts, which is, however, still controversial. Two major reaction mechanisms—redox and formate decomposition—have been proposed. The redox mechanism for the RWGS reaction can be simply modeled by the following scheme:



Cu⁰ atoms are apparently active to dissociate CO₂, while the reduction of oxidized Cu catalyst has to be faster than the oxidation process.^{49–51} Hydrogen is proposed to be a reducing reagent without direct participation in the formation of intermediates in the RWGS reaction. The other model based on the formate decomposition suggests that CO is formed from decomposition of formate intermediate, derived from the association of hydrogen with CO₂.^{35,52,53}

Chen *et al.* examined desorption energies of CO₂, active sites, and reaction mechanism of the RWGS reaction on Cu nanoparticles.⁵⁴ The Cu nanoparticles strongly bind CO₂ molecules, as evidenced by two main peaks with maxima at 353 K (α peak) and 525 K (β peak) in CO₂-TPD (temperature-programmed desorption of CO₂) spectra. β -Type CO₂ is substantiated as the major species for the RWGS reaction. Since an infrared band at 2007 cm⁻¹ was observed and assigned to CO adsorbed on low-index copper facets, the authors proposed that reaction pathways mainly include the formation of the formate species.^{55,56}

Different mechanisms have also been proposed for the reaction over Pd- and Pt-based catalysts. In a study using Pd/Al₂O₃ catalysts and supercritical mixture of CO₂ and H₂, infrared spectra indicated the formation of surface species such as carbonate, formate, and CO.⁵⁷ However, only carbonate and formate were observed on a bare alumina support. This contrast deduces that Pd facilitates the dissociative adsorption of H₂ and the formation of formates and CO. Another proposed mechanism over Pt/Al₂O₃ is shown in Scheme 2 based on the results acquired from *in situ* attenuated total reflection infrared spectroscopy (ATR-IRS).⁵⁸ The reaction of CO₂ and hydrogen takes place at the interface between Pt and Al₂O₃, and formed CO could serve as a probe molecule for the boundary sites. CO₂ adsorbs on oxygen defects of Al₂O₃ thin



Scheme 2 Schematic representation of the proposed mechanism of CO₂ reduction on a Pt/Al₂O₃ model catalyst. Red, white, and green balls depict carbon, oxygen, and hydrogen atoms, respectively. Reproduced with permission from ref. 58. Copyright 2002 Royal Society of Chemistry.

film to form carbonate-like species, and then reacts with hydrogen to form CO.

In order to dynamically identify the surface species over a Pt/CeO₂ catalyst, Goguet *et al.* developed a detailed spectrokinetic analysis monitored by diffuse reflectance Fourier transform infrared spectroscopy (DRIFT) and mass spectrometry (MS) using steady-state isotopic transient kinetic analysis (SSITKA).⁵⁹ A reaction model involving three kinds of mechanism is proposed in Fig. 1. Both of the formates and Pt-bound carbonyls species were observed, but neither of them was the main reaction intermediate, although the formation of CO from formates was likely to occur to a limited extent. The RWGS reaction proceeds mainly *via* surface carbonate intermediates, including reaction between the surface carbonates and oxygen vacancies or the diffusion of the vacancies in the ceria.⁵⁹

Theoretical investigations using model systems can also shed some light on the nature of molecular interactions. Qin *et al.* investigated the mechanism of the RWGS reaction on a Ni surface using density functional theory (DFT) calculations and predicted that the C–O bond cleavage of CO₂ occurred before the dissociation of the H₂.⁶⁰ The H₂ moiety could promote the charge transfer in the Ni insertion process and facilitate the dissociation of coordinated CO₂ molecule by reducing the energy barrier. The rate-determining step for the reaction is the migration of hydrogen atom from Ni center to oxygen atom with the formation of water.

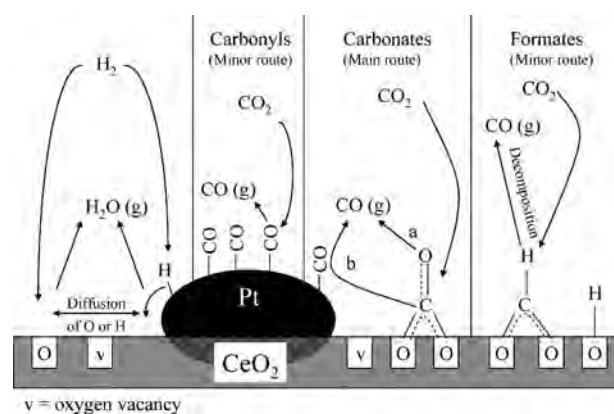


Fig. 1 Model for the reaction mechanism of the RWGS reaction over Pt/CeO₂. Reproduced with permission from ref. 59. Copyright 2004 American Chemical Society.

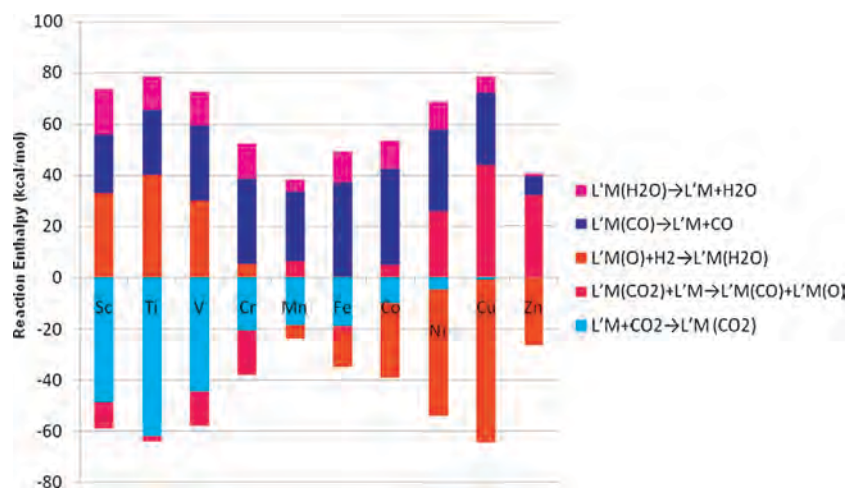
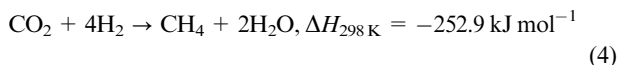


Fig. 2 Reaction enthalpies (kcal mol^{-1}) for each metal based enthalpies calculations. Reproduced with permission from ref. 61. Copyright 2010 American Chemical Society.

Liu *et al.* reported the modeling of the reaction mechanism for the RWGS reaction with first-row transition metal catalysts $L'M$ ($L' = \text{C}_3\text{N}_2\text{H}_5^-$; $M = \text{Sc, Ti, V, Cr, Mn, Fe, Co, Ni, Cu, Zn}$).⁶¹ The first step of catalytic reaction is the coordination of a CO_2 molecule ($L'M(\text{CO}_2)$). The second step is the scission of $L'M(\text{CO}_2)$ to produce $L'M(\text{CO})$ and $L'M(\text{O})$ by adding $L'M$, which is followed by hydrogenation of the oxo complex $L'M(\text{O})$ to generate $L'M(\text{H}_2\text{O})$. The last step involves dissociation of H_2O and CO . Reaction enthalpies for all the steps are depicted in Fig. 2. For catalytic cycle of the RWGS reaction, the key discriminating steps are the coordination and reduction of CO_2 . Early metals show a thermodynamic favor in these steps; however, late metals are more feasible for the hydrogenation of oxo complex.⁶¹

3. Methanation of carbon dioxide

Catalytic hydrogenation of CO_2 to methane, also called the Sabatier reaction, is an important catalytic process.



The methanation of CO_2 has a range of applications including the production of syngas and the formation of compressed natural gas. Research is being conducted by the National Aeronautics and Space Administration on the application of this reaction in manned space colonization on Mars.⁶² It is possible to convert the Martian CO_2 atmosphere into methane and water for fuel and astronaut life-support systems.⁶³

The methanation of CO_2 is thermodynamically favorable ($\Delta G_{298\text{K}} = -130.8 \text{ kJ mol}^{-1}$); however, the reduction of the

fully oxidized carbon to methane is an eight-electron process with significant kinetic limitations, which thus requires a catalyst to achieve acceptable rates and selectivities.⁶⁴ Extensive studies have been conducted on metal-based catalytic systems on the hydrogenation of CO_2 to methane.

3.1 Metal-based heterogeneous catalysts

Hydrogenation of CO_2 toward methane has been investigated using a number of catalytic systems based on VIIIIB metals (*e.g.*, Ru and Rh) supported on various oxides (*e.g.*, SiO_2 , TiO_2 , Al_2O_3 , ZrO_2 , and CeO_2). Supported nickel catalysts remain the most widely studied materials. Supports with high surface area, usually oxides, have been applied extensively for the preparation of metal catalysts. The nature of support plays a crucial role in the interaction between nickel and support, and thus determines catalytic performances toward activity and selectivity for CO_2 methanation.⁶⁵

Amorphous silica extracted from rice husk ash (RHA) has high specific surface area ($125\text{--}132 \text{ m}^2 \text{ g}^{-1}$), melting point, and porosity. Chang *et al.* reported that nickel catalysts supported on amorphous silica are active for methanation of CO_2 .^{66–68} Table 1 illustrates the turnover frequency (TOF) of methane (methane produced per nickel site per second) for hydrogenation of CO_2 on highly dispersed nickel catalysts prepared by various methods. Hydrogenation activity of nickel nanoparticles supported on amorphous silica is better than those on silica gel.⁶⁸

Amorphous silica is also used as a raw material for preparing a series of silica-alumina composites as supports for nickel-based catalysts ($\text{Ni/RHA-Al}_2\text{O}_3$) synthesized *via*

Table 1 Comparison of activities of CO_2 methanation on nickel catalysts

Catalyst	Preparation ^a	Dispersion (%)	T/K	TOF (10^3 s^{-1})	Ref.
4.3 wt% Ni/ SiO_2 -RHA	IE	40.7	773	17.2	68
4.1 wt% Ni/ SiO_2 -gel	IE	35.7	773	11.8	68
3.5 wt% Ni/ SiO_2 -RHA	DP	47.6	773	16.2	67
3.0 wt% Ni/ SiO_2	I	39.0	550	5.0	69

^a IE: ion exchange; DP: deposition-precipitation; I: impregnation.

ion exchange method.⁷⁰ It should be noted that reduction of NiO from the layered nickel compound is particularly difficult, which is probably due to the presence of alumina trapped in the NiO particles resulting in an increase in activation energy of reduction.⁷⁰ Conversion of CO₂ and yield of CH₄ are strongly dependent on the calcination and reduction temperatures of the catalysts. Hydrogenation activity decreases as content of alumina increases, indicating that acidic sites are not uniquely responsible for the reaction. Ni/RHA–Al₂O₃ catalyst was also prepared by the incipient wetness impregnation and exhibited favorable catalytic activity owing to the mesopores structure and high surface area.⁶⁵ A strong interaction between metal and oxide (SIMO) was found for this system. Consequently, nanocrystallites of nickel oxide (e.g., NiO and NiAl₂O₄) are formed with high dispersion on the surface. At an optimized reaction temperature (773 K), maximized yield (~58%) and selectivity of CH₄ (~90%) were obtained.⁶⁵ The catalytic activity of Ni/RHA–Al₂O₃ is better than that of Ni/SiO₂–Al₂O₃ due to its better metal dispersion and higher chemical reaction rate.

On account of significant influence of the support on dispersion of the active phase, preparation of highly dispersed metal supported catalysts has been the focus of research. Du *et al.* applied Ni/MCM-41 catalysts with different amount of Ni to CO₂ methanation.⁶³ High selectivity (96.0%) and space-time yield (STY, 91.4 g kg⁻¹ h⁻¹) were achieved on 3 wt% Ni/MCM-41 at a space velocity of 5760 kg⁻¹ h⁻¹, superior to those of Ni/SiO₂ catalysts and comparable to Ru/SiO₂ catalysts.^{69,71,72} The high selectivity is maintained at higher reaction temperature (673 K) with increased STY (633 g kg⁻¹ h⁻¹). Reduction at 973 K produces stable catalyst yielding the best activity and selectivity since most Ni species is reduced to highly dispersed Ni⁰ due to the surface anchoring effect.⁶³

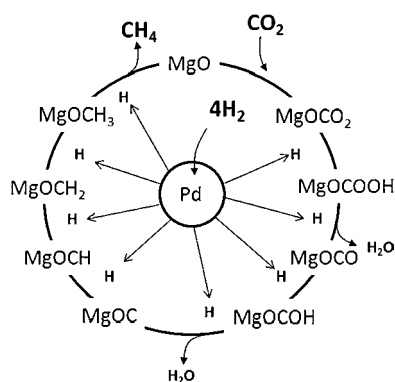
ZrO₂ is another support of interest due to its acidic/basic features and CO₂ adsorption abilities. Ni/ZrO₂ catalysts with various amounts of ZrO₂ polymorph can be prepared from amorphous Ni–Zr alloys.⁷³ Fraction of tetragonal ZrO₂ (*t*-ZrO₂) increases with increasing nickel content, which subsequently influences the methanation activity. Nickel nanoparticles supported on *t*-ZrO₂ show a higher TOF (5.43 s⁻¹ at 473 K) and better CO₂ adsorption than those loaded on the monoclinic ZrO₂ (*m*-ZrO₂) (0.76 s⁻¹ of TOF at 473 K).⁷³ Ce–Zr binary oxides have also been used in CO₂ methanation as supporting materials for supplying oxygen species with high mobility. Ocampo *et al.* studied Ni/Ce_{0.72}Zr_{0.28}O₂ catalysts for the synthesis of methane.⁷⁴ A catalyst with 10 wt% Ni exhibits excellent catalytic activity and stability in the reaction during 150 h on stream, yielding a CO₂ conversion and a CH₄ selectivity of 75.9% and 99.1%, respectively. The high oxygen storage capacity of Ce_{0.72}Zr_{0.28}O₂ and its ability to enhance nickel dispersion is the origin of the high performance. The incorporation of nickel cations into the Ce_{0.72}Zr_{0.28}O₂ structure and the higher dispersion of Ni improve redox properties of the material, and thus restrain sintering of the metal. Additionally, Perkasa *et al.* developed Ni/ZrO₂ catalysts doped with Ce or Sm cation.⁷⁵ The maximum porous volume and size are obtained with 30 mol% Ni loading, which exhibits higher catalytic activity of CO₂ methanation

(1.5 s⁻¹ of TOF at 573 K). This could be ascribed to a synergistic effect between the surface area and the doping of the rare earth elements. The surface area of the catalyst is increased due to the mesopores structure in the support, which leads to the insertion of the Ni particles into the pores. The catalytic activity could be further improved by a redox pretreatment.⁷⁵

We certainly need to recall RANEY[®] nickel, which is well-known as an active catalyst for hydrogenation and appears to have high reactivity in the methanation reaction.⁷⁶ The notable catalytic performance is attributed to its unique thermal and structural stability as well as a large BET surface area. Main products were observed to be CH₄ and CO over Ni–Al alloys.⁷⁷ An increase in Ni content leads to higher selectivity to methane (100%), since Ni (compared to Al) readily dissociates CO. Moreover, a series of mono- and bi-metallic Ni-based catalysts supported on alumina were examined *via* a computational screening study.⁷⁸ The conversion of CO₂ to methane is significantly increased over Ni–Fe alloy compared to the pure nickel or iron catalyst, and the best catalyst has a Ni/Fe ratio higher than 1.

One of major problems of Ni-based catalysts is the deactivation at low temperature due to the interaction of the metal particles with CO and formation of mobile nickel subcarbonyls.⁷⁹ Instead, noble metal (e.g. Ru, Pd, and Pt) is stable at operating conditions and more active for CO₂ methanation than nickel.⁸⁰ Kowalczyk *et al.* studied the effect of the support on catalytic properties of Ru nanoparticles in CO₂ hydrogenation.⁸¹ They found that TOFs of Ru-based catalysts were dependent on the Ru dispersion and the type of supports. For high metal dispersion, the following order of TOFs (×10³ s⁻¹) for the reaction was obtained: Ru/Al₂O₃ (16.5) > Ru/MgAl₂O₄ (8.8) > Ru/MgO (7.9) > Ru/C (2.5).⁸¹ The catalytic activity of ruthenium nanoparticles is strongly affected by the metal-support interaction. In the case of Ru/C systems, the carbon moiety partially covers the metal surface and reduces the number of active sites (*i.e.*, site blocking effect).⁸¹ Under steady-state conditions, reaction rate of a highly loaded 15 wt% Ru/Al₂O₃ is about 10 times higher than that of Ni-based catalysts. Highly dispersed Ru nanoparticles were also synthesized on TiO₂ prepared by a barrel-sputtering method.⁸² Remarkably, a 100% yield was achieved over this catalyst at 433 K, which was significantly higher compared to that prepared by conventional wet impregnation. The prepared Ru/TiO₂ sample can catalyze the methanation reaction at low temperature (300 K) with a reaction rate of 0.04 μmol min⁻¹ g⁻¹. Furthermore, the addition of yttrium to Ru-based catalysts not only increases the active surface area and the dispersion of ruthenium but also benefits catalytic activity and anti-poisoning capacity of the catalysts.⁸³ Ru/γ-Al₂O₃ was also used as a probe catalyst to determine kinetic parameters for CO₂ methanation.⁸⁴ Apparent activation energy reaches a minimum (82.6 kJ mol⁻¹) at a ruthenium dispersion of 50%. Reaction order with respect to hydrogen decreases with the increase of H/Ru ratio, which could be attributed to a change in adsorption heat of hydrogen and an increased number of low-coordination sites.

Park *et al.* have investigated bifunctional Pd–Mg/SiO₂ for CO₂ methanation motivated by the property of Pd to



Scheme 3 Potential bifunctional model for Pd–Mg/SiO₂. Reproduced with permission from ref. 64. Copyright 2009 Elsevier.

dissociate molecular hydrogen.⁶⁴ At 723 K, the Pd–Mg/SiO₂ catalyst shows a high selectivity (>95%) to CH₄ with 59% of CO₂ conversion, whereas Pd supported on silica reduces CO₂ primarily to CO whereas Mg/SiO₂ alone is inactive. A bifunctional mechanism was proposed that Pd provides disassociated hydrogen to Mg carbonates to form methane, and upon the desorption of the methane, the carbonate is reformed by gas phase CO₂ (Scheme 3).⁶⁴

Recently, platinum supported on titania nanotubes (Pt/Tnt) with high surface area (187 m² g⁻¹) has been prepared.⁸⁵ The catalyst contains scrolled multi-walled titania-nanotubes uniformly dispersed with Pt nanoparticles in the mixed-valence states. CO₂-TPD results indicated that a large amount of CO₂ adsorbed on the Pt/Tnt is ascribed to the combined effect of the tubular structure with high surface area and Pt nanoparticles with the mixed-valence. *In situ* FTIR demonstrated that CH₄ was the unique product during the reaction and Pt/Tnt catalyst showed high activity for CO₂ methanation at low temperature (450 K).

Since industrial feedstock typically contains a trace amount of sulfur compounds, Szailer *et al.* have examined the effect of sulfur on the methanation of CO₂.⁸⁶ Interestingly, a trace amount of H₂S (*e.g.*, 22 ppm) can promote the reaction on TiO₂- and CeO₂-supported metals clusters (*e.g.*, Ru, Rh, and Pd), whereas, on other supported catalysts (*e.g.*, ZrO₂- and MgO-based) or when the H₂S content is high (116 ppm), the reaction rate decreases. When the support is diffused with H₂S, the catalyst becomes more activity as a result of the formation of new active sites at interfaces between the metal and the support.⁸⁶

Most of the catalytic methanation of CO₂ have been performed in fixed-bed reactors. However, the utilization of electrochemistry in the reactor design is cost efficient and environmentally friendly to industrial processes with a minimum of waste production and toxic materials.⁸⁷ CO₂ hydrogenation using YSZ solid electrolyte and Rh electrode was studied in a single chamber reactor.⁸⁸ CO and CH₄ were produced at temperatures of 346–477 °C, and the rates of CH₄ and CO formation were enhanced with positive potentials (electrophobic behavior) and negative potentials (electrophilic behavior), respectively. Moreover, a monolithic electro-promoted reactor (MEPR) with Rh/YSZ/Pt or Cu/TiO₂/YSZ/Au cells was used to investigate the hydrogenation of CO₂ at atmospheric pressure.⁸⁹ In the case of Rh/YSZ/Pt cells,

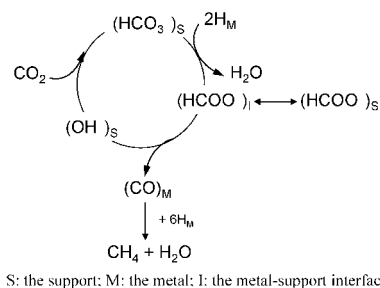
both positive and negative applied potentials significantly enhance the total hydrogenation rate and the formation of CO, but the selectivity of CH₄ remains below 12%. In the case of Cu/TiO₂/YSZ/Au cells, selective reduction of CO₂ to CH₄ starts at 220 °C and the selectivity of CH₄ could reach ~100% at open-circuit polarization conditions at temperatures of 220–380 °C.⁸⁹

3.2 Reaction mechanism

Although the methanation of CO₂ is a comparatively simple reaction, its reaction mechanism appears to be difficult to establish. There are different opinions on the nature of the intermediate and the methane formation process. Reaction mechanisms proposed for CO₂ methanation fall into two main categories. The first one involves the conversion of CO₂ to CO prior to methanation, and the subsequent reaction follows the same mechanism as CO methanation.^{90–94} The other one involves the direct hydrogenation of CO₂ to methane without forming CO as intermediate.^{95,96} We note that, even for CO methanation, there is still no consensus on the kinetics and mechanism. It has been proposed that the rate-determining step is either the formation of the CH_xO intermediate and its hydrogenation or the formation of surface carbon in CO dissociation and its interaction with hydrogen.^{94,97}

Steady-state transient measurements have been employed in kinetic investigations on a Ru/TiO₂ catalyst to identify reaction intermediates.⁹³ CO is a key intermediate and its hydrogenation leads to the formation of methane. Formates, also as intermediates for the formation of CO, are bound more strongly on the support in equilibrium with the active formate species on the interface between metal and support. A reaction mechanism (Scheme 4) is proposed including the formation of the formate through a carbonate species.

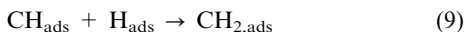
A surface science approach using model systems is considerably helpful in understanding mechanistic aspects of reactions. Ni single crystals have been shown to be reasonable models of practical catalysts for methanation.^{98,99} Peebles *et al.* studied the methanation and dissociation of CO₂ on Ni(100).⁷¹ Activation energies of 88.7 kJ mol⁻¹ and 72.8–82.4 kJ mol⁻¹ were acquired for the formation of CH₄ and CO, respectively. The activation energy and reaction rate for CO₂ methanation are very close to values for CH₄ formation from CO under identical reaction conditions. The results support a mechanism that CO₂ is converted to CO and subsequently to carbon before hydrogenation. Using the ASED-MD (atom superposition and electron delocalization-molecular orbital) theory,



S: the support; M: the metal; I: the metal-support interface.

Scheme 4 Proposed reaction mechanism for CO₂ methanation. Reproduced with permission from ref. 93. Copyright 1997 Elsevier.

Choe *et al.* investigated the CO₂ methanation on a Ni(111) surface in a detailed manner.¹⁰⁰ The elementary reaction steps are listed below.



These elementary steps consist of two mechanisms—carbon formation and carbon methanation. For the first mechanism, the activation energies were calculated to be 1.27 eV for CO₂ dissociation, 2.97 eV for the CO dissociation, and 1.93 eV for the 2CO dissociation. For the carbon methanation mechanism, following activation energies were reported: 0.72 eV for methylidyne, 0.52 eV for methylene, and 0.50 eV for methane.¹⁰⁰ Thus, CO dissociation is the rate-determining step.

In aiming to provide clear insights into the role of Pd and MgO, Kim *et al.* used computational and experimental methods investigating the reaction mechanism of CO₂ methanation on Pd–MgO/SiO₂.¹⁰¹ CO₂-TPD results agree with DFT calculations that MgO initiates the reaction by binding CO₂ molecules, forming an activated surface magnesium carbonate species. Pd species dissociates molecular hydrogen, essential for further hydrogenation of the carbonates and residual carbon atoms. The bifunctional reaction mechanism is consistent with the previously proposed reaction scheme (Scheme 3).⁶⁴

Interestingly, it has been demonstrated that CO₂ can react with H₂ over Rh/γ-Al₂O₃ catalyst to produce methane at room temperature and atmospheric pressure with a high selectivity (99.9–100%), even without photoexcitation.¹⁰² Jacquemin *et al.* looked into the reaction mechanism of CO₂ methanation on the Rh/γ-Al₂O₃ catalyst to better understand this process.¹⁰³ The dissociation of CO₂ into CO and oxygen on the surface of the catalyst has been evidenced *via in situ*

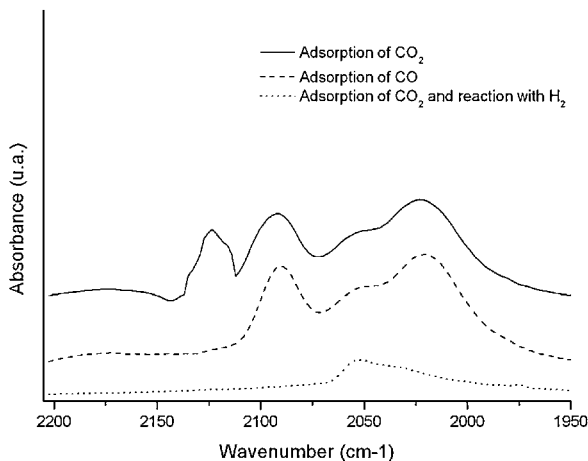


Fig. 3 DRIFT results after adsorption of CO₂ and CO and after adsorption of CO₂ and reaction with hydrogen. Reproduced with permission from ref. 103. Copyright 2010 Elsevier.

DRIFT experiments (Fig. 3). The formation of CO_{ads} was confirmed by the presence of the bands corresponding to linear Rh–CO (2048 cm⁻¹), Rh³⁺–CO (2123 cm⁻¹), and Rh–(CO)₂ (2024 and 2092 cm⁻¹). CO₂ adsorbed as Rh–(CO)₂ and CO associated with oxidized Rh are the most reactive species with hydrogen.

4. Synthesis of hydrocarbons

Production of hydrocarbons from CO₂ hydrogenation is essentially a modification of the Fischer–Tropsch (FT) synthesis, where CO₂ is used instead of CO. Catalyst component for CO₂ hydrogenation is analogous to that for FT synthesis but is amended to maximize the production of hydrocarbons. A number of studies have been carried out on this subject, which can be divided into two categories—methanol-mediated and non-methanol-mediated reactions.^{104,105} In the methanol-mediated approach, CO₂ and H₂ react over Cu–Zn-based catalysts to produce methanol, which is subsequently transformed into other hydrocarbons such as gasoline.¹⁰⁶ In spite of considerable efforts made in the development of composite catalysts, this approach usually yields light alkanes as major products owing to the further catalytic hydrogenation of the alkenes.¹⁰⁷ In the case of non-methanol-mediated process, CO₂ hydrogenation proceeds *via* two steps—RWGS reaction and FT synthesis.

Cobalt catalysts are widely used in FT synthesis, owing to the high performance-to-cost ratio. Upon switching feeding gas from syngas to the gas mixture of CO₂ and H₂, cobalt performs as a methanation catalyst rather than acting as an FT catalyst.^{108–111} Mixed Fe/Co catalysts have also exhibited low selectivity to the desired hydrocarbons.¹¹² Akin *et al.* observed that products of CO₂ hydrogenation contain ~70 mol% methane over Co/Al₂O₃ catalyst.¹¹⁰ They proposed that the conversion of CO and CO₂ occurs *via* different reaction pathways: the former involving mainly species of C–H and O–H produced from hydrogenation, the latter involving surface-bound intermediates of H–C–O and O–H.¹¹⁰ In order to better clarify the difference in product distributions of CO and CO₂ hydrogenation, Fig. 4 shows

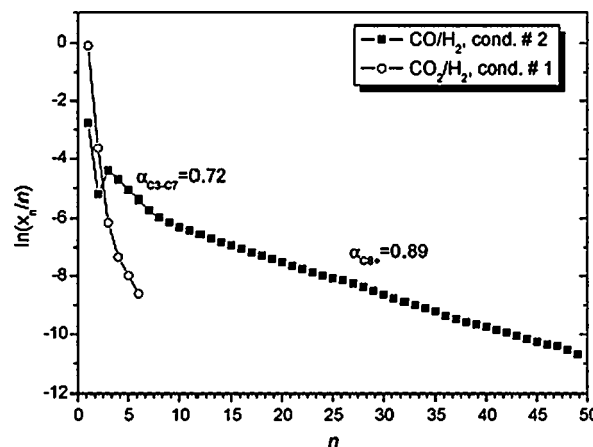
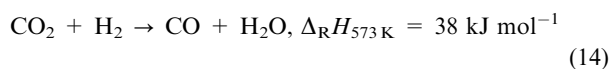


Fig. 4 ASF plots in terms of hydrocarbons selectivity during CO and CO₂ hydrogenation. Reproduced with permission from ref. 113. Copyright 2009 Elsevier.

typical Anderson-Schulz-Flory (ASF) diagrams in terms of selectivity of total hydrocarbons in CO and CO₂ hydrogenation.¹¹³ It is obvious that hydrogenation of CO₂ does not lead to a typical ASF distribution, different from what takes place for CO hydrogenation. During CO₂ hydrogenation a low C/H ratio is obtained due to the slow CO₂ adsorption rate on the surface. This favors the hydrogenation of surface-adsorbed intermediates, leading to formation of methane and a decrease in chain growth.

Iron oxides have been used as FT catalysts for many years, which are also active in both WGS and RWGS reactions.^{114–116} Iron-based catalysts are attractive for the synthesis of hydrocarbons due to the highly olefinic nature of the obtained products.^{117–119} CO₂ hydrogenation over an iron catalyst proceeds *via* a two-step process, with initial reduction of CO₂ to CO *via* the RWGS reaction followed by the conversion of CO to hydrocarbons *via* a FT reaction.^{120–123}



Riedel *et al.* demonstrated that the steady states of hydrocarbons synthesis with iron oxides could be divided into five episodes of distinct kinetic regimes (Fig. 5).^{124,125} In episode I, the reactants adsorb on the catalyst surface and carbonization of the catalyst takes place dominantly. In episodes II and III, products from the RWGS reaction dominate during ongoing carbon deposition. In episode IV, the FT activity develops up to the steady state and keeps the state in episode V. The iron phases of the reduced catalyst before reaction consist of mainly α -Fe and Fe₃O₄. With time, Fe₃O₄ and Fe₂O₃ phases are consumed and a new amorphous, probably oxidic, iron phase is formed, which appears to be active for the RWGS reaction. FT activity begins under the formation of iron carbide (Fe₅C₂) by a reaction of iron with carbon from CO dissociation. We also need to mention that iron-based catalysts deactivate significantly during CO₂ hydrogenation because of catalyst poisoning from carbon deposit.¹⁰⁶ For example, the deactivation occurs on a Fe–K/ γ -Al₂O₃ catalyst in a packed bed reactor although the long-run activity is above

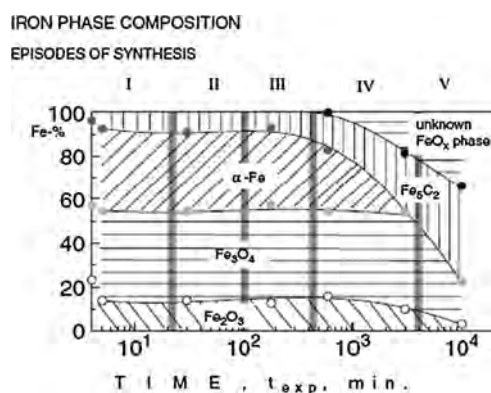


Fig. 5 Iron-phase composition as a function of time during hydrocarbons synthesis on Fe/Al/Cu catalyst. Reproduced with permission from ref. 125. Copyright 2003 Springer.

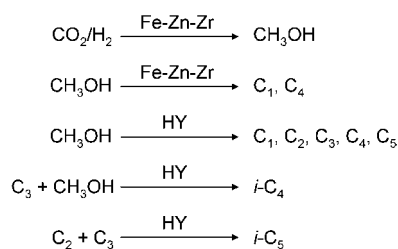
35% during the reaction.¹²⁶ The stable but inactive carbide (Fe₃C) is accountable for the deactivation of the catalyst, which is formed by Fe₅C₂ carburization.¹²⁶

In order to increase the yield of the desired hydrocarbons products, promoters are often added to catalysts to tailor and optimize product distribution. Potassium is a favorable promoter and has significant influence on catalytic performance.^{106,127–129} Addition of potassium not only leads to a significant shift in olefin production (4-fold) but also an increase in CO₂ conversion.¹³⁰ In addition to be present in the oxide form, potassium could also form an alanate phase (KAlH₄), which has recently attracted much attention for its ability of reversible hydrogen storage at high temperature. Potassium acts as an electronic promoter to the iron, as well as suppresses the hydrogenation of the products as a reversible H₂ reservoir.¹³⁰ For example, K/Mn/Fe-based catalyst displays a high chain growth.^{111,130,131}

Manganese acts as both structural promoter and electronic modifier for iron-based catalysts. The addition of Mn suppresses the formation of methane and increases the ratio of olefin/paraffin in FT synthesis as well as CO₂ hydrogenation.^{130,132,133} It has been suggested that Mn favors the reduction of iron oxides and the carburization and dispersion of Fe₂O₃, and also greatly increases surface basicity of the catalyst.^{128,134} However, over-doping of Mn on the iron catalyst reverses the promotional effect, leading to the suppression of the desirable hydrocarbon products.¹³⁰ Copper can also significantly enhance CO₂ hydrogenation reactivity owing to its similar performance with Mn in nature.^{129,135} Copper facilitates the reduction of the catalyst and provides active sites for hydrogen dissociation.¹²⁸

Ceria is highly active in the WGS reaction at low temperature, and thus is of immense interest in applications such as fuel cells.¹³⁶ Ceria added to an iron catalyst has little effect on the conversion of CO₂ to hydrocarbons, but shortens the time of stationary-state operation conditions.¹³⁷ Although low loading of ceria to a Fe–Mn/Al₂O₃ catalyst leads to a marginal improvement in CO₂ conversion and product selectivity, a decrease in reactivity was observed when the doping amount is increased to 10 wt%.¹³⁸ Ceria particles are formed over iron nanoparticles causing the blocking of the chain-growth sites. Other additives including Zr, Zn, Mg, Ru, and La have also been investigated but promoting effect is nearly negligible.^{106,127,129,139–142}

Iron-based catalysts dispersed on different supports have also been examined extensively and the product distributions are greatly dependent on supporting materials.¹⁰⁶ The support tends to act purely as a stabilizer to avoid sintering of active particles during the reaction. Generally, alumina performs best, since it could prevent sintering as a result of the strong metal-support interaction, followed by silica and titania.^{106,111,143,144} Zeolites have surface characteristics of pore structures and inner electric fields, resulting in different catalytic performances. Effects of the type of zeolites on catalytic activity for synthesis of isoalkanes from CO₂ hydrogenation were investigated over Fe–Zn–Zr/zeolite catalysts.¹⁴⁰ Distribution of hydrocarbon products is influenced by the structure and acidity of the zeolites.¹⁴⁵ HY zeolite is most effective for isoalkane synthesis due to the presence of medium



Scheme 5 Reaction paths of isoalkanes formation over Fe–Zn–Zr/HY catalyst. Reproduced with permission from ref. 139. Copyright 2007 Elsevier.

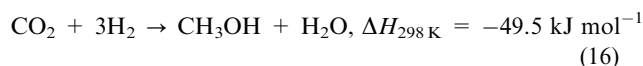
and strong acid sites. Reaction paths of isoalkanes formation over a Fe–Zn–Zr/HY catalyst (Scheme 5) indicate that methanol is synthesized directly from CO₂ hydrogenation, and the RWGS reaction is not the indispensable step for hydrocarbons formation.¹³⁹ The *i*-C₄ (*iso*-butane) can be obtained from propylene and methanol through methanol to gasoline (MTG) reaction and *i*-C₅ (*iso*-pentane) is formed from the reaction of C₂ and C₃ through the additive dimerization.¹³⁹

We should mention that the formed H₂O not only deactivates catalysts but also suppresses the reaction rate of CO₂ hydrogenation. An alternative approach to improve productivity of long chain hydrocarbons is the utilization of a permselective silica membrane to remove water *in situ*.^{146,147} Fluidized bed and slurry reactors have been employed to increase the conversion of CO₂ and obtain desirable products as they are beneficial for the removal of generated heat due to the highly exothermic nature of the reaction.¹⁴⁸ Hydrogenation of CO₂ to hydrocarbons proceeded in fluidized bed and slurry reactors over Fe–Cu–Al–K catalyst yields better catalytic performance compared to a fixed bed reactor.¹⁴⁸ Moreover, light olefins and heavy hydrocarbons can be selectively formed in fluidized bed reactors and slurry reactors, respectively.

5. Synthesis of methanol

Methanol is a common solvent, an alternative fuel, and a starting material in chemical industry. As an alternative

feedstock, CO₂ has replaced CO and is considered as an effective way for CO₂ utilization in the methanol production.¹¹



From the thermodynamic point of view, a decrease in reaction temperature or an increase in reaction pressure could favor the synthesis of methanol. Indeed, enhanced reaction temperature (*e.g.*, higher than 513 K) facilitates CO₂ activation and subsequent methanol formation.¹¹ Furthermore, other by-products are formed during the hydrogenation of CO₂, such as CO, hydrocarbons, and higher alcohols.¹⁴⁹ Therefore, a highly selective catalyst is in need to avoid the formation of undesired by-products for methanol synthesis. Typically, catalysts used in CO₂ hydrogenation are those for methanol synthesis from CO hydrogenation. A number of investigations have addressed the effects of active components, supports, promoters, preparation methods, and surface morphology on reactivity.

5.1 Reactivity and structure of heterogeneous catalysts

Although many kinds of metal-based catalysts have been examined for the synthesis of methanol, Cu remains the main active catalyst component, together with different modifiers (Zn, Zr, Ce, Al, Si, V, Ti, Ga, B, Cr, *etc.*).^{150–152} An appropriate support not only affects the formation and stabilization of the active phase of the catalyst but also is capable of tuning the interactions between the major component and promoter. In addition, basicity and/or acidity characteristics of the catalyst are also determined by the selected support.¹⁵³ The status of catalytic systems for the synthesis of methanol by CO₂ hydrogenation is summarized in Table 2.

Notably, zinc oxide can improve the dispersion and stabilization of copper.^{167,168} ZnO possesses lattice oxygen vacancies, consisting of an electron pair in the lattice, which is active for methanol synthesis.¹⁵³ Fujita *et al.* showed high activity and selectivity (67.2%) of methanol over a Cu/ZnO catalyst due to the high dispersion of Cu and the preferential

Table 2 Catalytic systems for the synthesis of methanol by the hydrogenation of CO₂

Catalyst	Preparation method	<i>T</i> /°C	CO ₂ conversion (%)	Methanol selectivity (%)	Methanol activity (mol kg ⁻¹ cat. h)	Ref.
Cu/Zn/Ga/SiO ₂	co-impregnation	270	5.6	99.5	10.9	154
Cu/Ga/ZnO	co-impregnation	270	6.0	88.0	11.8	155
Cu/ZrO ₂	deposition-precipitation	240	6.3	48.8	11.2	156
Cu/Ga/ZrO ₂	deposition-precipitation	250	13.7	75.5	1.9	157
Cu/B/ZrO ₂	deposition-precipitation	250	15.8	67.2	1.8	157
Cu/Zn/Ga/ZrO ₂	coprecipitation	250	n/a	75.0	10.1	158
Cu/Zn/ZrO ₂	coprecipitation	250	19.4	29.3	n/a	159
Cu/Zn/ZrO ₂	urea-nitrate combustion	240	17.0	56.2	n/a	160
Cu/Zn/ZrO ₂	coprecipitation	220	21.0	68.0	5.6	161
Cu/Zn/ZrO ₂	glycine-nitrate combustion	220	12.0	71.1	n/a	162
Cu/Zn/Al/ZrO ₂	coprecipitation	240	18.7	47.2	n/a	163
Ag/Zn/ZrO ₂	coprecipitation	220	2.0	97.0	0.46	161
Au/Zn/ZrO ₂	coprecipitation	220	1.5	100	0.40	161
Pd/Zn/CNTs	incipient wetness	250	6.3	99.6	1.1	164
G ₂ O ₃ -Pd/SiO ₂	incipient wetness	250	n/a	70.0	7.9	165
LaCr _{0.5} Cu _{0.5} O ₃	sol-gel	250	10.4	90.8	n/a	166

n/a: not available.

formation of flat Cu surfaces, such as Cu(111) and Cu(100).^{169,170} Ponce *et al.* prepared nanocrystalline (NC) particles of copper using solvated metal atom dispersion (SMAD) technique to convert CO₂ to CH₃OH.¹⁷¹ A maximum CO₂ conversion of 80% was obtained for the Cu/pentane/NC-ZnO sample at 450 °C.

In order to further increase the activity and stability of Cu/ZnO catalyst, Ga₂O₃ and SiO₂ are used as stabilizer and promoter.¹⁵⁴ The promoting effect of Ga₂O₃ is strongly associated with Ga₂O₃ particle size. Small Ga₂O₃ particles favor the formation of an intermediate state of copper between Cu⁰ and Cu²⁺, probably Cu⁺.^{154,155} Toyir *et al.* found that the use of methoxide-acetylacetonate precursor for preparation of a Cu-Ga/ZnO catalyst yields a better dispersion of copper compared to catalyst prepared from nitrate precursor.¹⁵⁵ SiO₂-supported multicomponent catalysts, especially when hydrophobic silica is used, are effective and fairly stable for the production of methanol at temperature up to 270 °C.¹⁵⁴ Noble metals are excellent candidates to activate hydrogen, which could spread over the neighboring sites through a hydrogen-spillover mechanism. Pd is used to modify the Cu/ZnO or Cu/Zn/Al₂O₃ catalysts for CO₂ hydrogenation to methanol.^{172,173} This process leads to a catalyst surface with highly reduced state, which could facilitate the hydrogenation process.¹⁷²

Because of the high stability under reducing or oxidizing atmospheres, zirconia has also been considered as an excellent promoter or support for the methanol synthesis catalyst.^{151,156,163} Catalytic activity and selectivity toward methanol are both improved due to the enhanced copper dispersion in the presence of ZrO₂.^{151,159,160,174,175} In addition, the crystal types of zirconia influence performance of the catalyst.^{162,176} For instance, copper species supported on *m*-ZrO₂ are 4.5 times more active compared to Cu/*t*-ZrO₂ due to the higher concentration of adsorbed active intermediates (*i.e.*, HCOO and CH₃O).¹⁷⁶ Addition of other components (*e.g.*, Ga, B, and Al) not only decreases the adsorption rate of water which inhibits the formation of methanol but also improves the copper dispersion and ZrO₂ concentration on the surface, leading to an increase of catalyst activity.^{152,157,158,177} A simplified mechanism of the catalyst surface and reaction paths is proposed in Scheme 6.¹⁷⁴ CO₂ adsorbed on the surface of ZrO₂ forms a bicarbonate species, which is then hydrogenated to produce formate intermediate species.¹⁷⁸ Hydrogen required for the formation of formate species could be provided by the spillover of adsorbed hydrogen on Cu.^{166,179}

In addition to Cu-based catalysts, several other materials exhibit activity in CO₂ hydrogenation. For example, Ag- and Au-based catalysts offer superior selectivity with high content of metal.¹⁶¹ Pd/ZnO catalysts supported on multi-walled

carbon nanotubes (MWCNTs) exhibit excellent performance for the formation of methanol owing to an increasing concentration of active Pd⁰ species.¹⁶⁴ MWCNTs-supported Pd/ZnO catalysts could reversibly adsorb enhanced amount of hydrogen, which favors for the generation of a micro-environment with higher concentration of active hydrogen species and increases the reaction rate of the surface hydrogenation. Pd/Ga₂O₃ catalyst reveals remarkable activity and selectivity in the methanol synthesis owing to the formation of new active sites by Pd-Ga alloy.¹⁸⁰ Hydrogen dissociated on metallic Pd surface transfers to Ga₂O₃ and reacts with surface-bound species (*e.g.*, formates) completing the reaction cycle.^{165,181}

It is interesting that formaldehyde rather than methanol is the main product when the reaction is carried out over a Pt/Cu/SiO₂ catalyst at 423 K and 0.6 MPa.¹⁸² The optimal atomic ratio of Pt/Cu for the selective formation of formaldehyde is 0.03. Hydrogen is chemisorbed on the surface of platinum, and then diffuses to the surface of copper. The migrated surface hydrogen promotes the formation of formaldehyde.

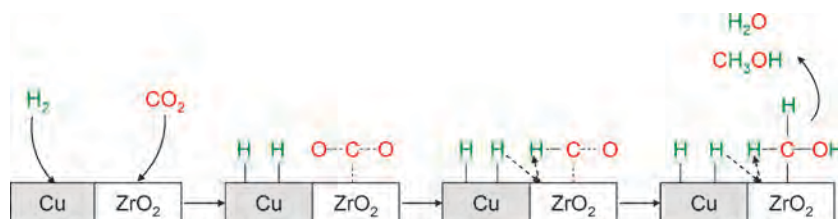
5.2 Non-metal-mediated homogeneous catalysts

Stephan and co-workers have recently developed a concept called “frustrated Lewis pairs” (FLPs).¹⁸³ In the system, a strong donor–acceptor interaction is prevented by the steric environment imposed on substitutional donor and acceptor atoms. The system can be used in metal-free homogeneous hydrogenation or addition to olefins and other organic chemicals.^{184–186} Ashley *et al.* performed the heterolytic activation of hydrogen and subsequent insertion of CO₂ into a B–H bond in a homogeneous process for the synthesis of methanol (Scheme 7).¹⁸⁷ Methanol (17–25% of yield) as the sole C₁ product was generated by adding CO₂ to 2,2,6,6-tetramethylpiperidine (TMP, Me₄C₅NH) and B(C₆F₅)₃ in toluene under H₂ (1–2 atm), upon heating the mixture at 160 °C and vacuum distillation.¹⁸⁷

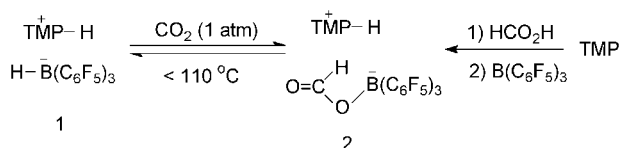
5.3 Reactor design and optimization

The yield and selectivity of methanol are usually low using traditional fixed-bed tubular reactors. Rahimpour proposed a two-stage catalyst bed for conversion of CO₂ into methanol, which favors the temperature profile along the reactor tube length and enhances the activity and life time of the catalyst.¹⁸⁸ Additionally, the same group investigated the hydrogenation of CO₂ in a membrane dual-type reactor.¹⁸⁹ This type of reactor can overcome limitation of thermodynamic equilibrium, enhance kinetics-limited reactions, and control the stoichiometrical feeds.¹⁹⁰

Owing to the ability of removing products continuously from equilibrium reaction, more researchers have focused on



Scheme 6 Proposed reaction pathway for the formation of methanol over CO₂ hydrogenation with Cu/ZrO₂ catalyst.



Scheme 7 Reversible reduction of CO₂ to formate 2 with H₂ activated by a frustrated Lewis acid–base pair 1. Reproduced with permission from ref. 187. Copyright 2009 Wiley-VCH Verlag GmbH & Co. KGaA.

the utilization of membrane reactor (MR) in methanol production. From an experimental and modeling study, MR exhibits higher conversion than the traditional fixed bed reactor under the same experimental conditions.¹⁹¹ However, the application of MR is limited by the working temperature typically below 200 °C. Chen *et al.* simulated methanol synthesis from CO₂ in a silicone rubber/ceramic composite MR and coupling with experimental data demonstrated that conversion of the main reaction in MR increases by 22% compared to the traditional fixed bed reactor.¹⁹² Additionally, many research groups have revealed the improvement in methanol selectivity and yield in MR with different kinds of membrane (*e.g.*, ceramic zeolite).^{193–195}

In order to overcome thermodynamics limitation, low-temperature methanol synthesis in liquid medium has been intensely studied.¹⁹⁶ The process has the advantages of high heat transfer efficiency, high conversion per run, excellent adaptability to CO₂, and low operation cost.^{197–200} Liaw *et al.* explored ultrafine copper boride catalysts (Me–CuB (Me: Cr, Zr, Th)) for the CO₂ hydrogenation in the liquid-phase.¹⁵⁰ The doping of Cr, Zr, and Th promotes the dispersion and stability of the CuB catalyst, and facilitates methanol formation. Liu *et al.* developed a novel low-temperature route in a semi-bath autoclave reactor for the synthesis of methanol over copper catalyst.²⁰¹ This process realizes a high catalytic activity of CO₂ conversion (25.9%) and methanol selectivity (72.9%) at low temperature (170 °C) and pressure (5 MPa).

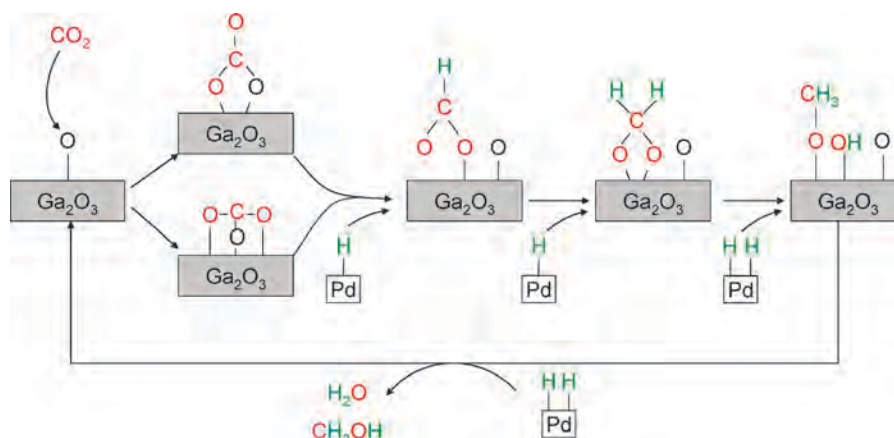
5.4 Theoretical studies

Owing to great complexity of methanol synthesis from CO₂ hydrogenation, atomic level understanding regarding the

reaction mechanism has been a long-standing challenge. Up to now, the key issues in the field, such as how and where CO₂ is activated over the surface of the catalysts, remain elusive.¹⁵³ The synthesis of methanol is generally regarded as occurring at interfaces of Cu and oxides.^{96,202} In other words, CO₂ can adsorb on bare oxides and H₂ can dissociate on Cu species.¹⁷⁸ However, the nature of the active Cu phase at interface is still in dispute. Köeppel *et al.* found that active copper species is present predominantly as Cu⁰ over Cu/ZrO₂ based on X-ray diffraction (XRD) measurements.²⁰³ In contrast, Cu⁺ was proposed to be the active component for a Cu/ZnO/SiO₂ catalyst employing static low-energy ion scatter experiments.²⁰⁴ However, it has also been suggested that Cu metal and low valence of Cu (Cu^{δ+} and Cu⁺) may all affect the catalytic activity of Cu-based oxide catalysts.^{156,157,205,206} Resolution of the electronic and geometrical structures of the active site is the first step towards the rational design of catalyst with high activity and selectivity.²⁰⁷

Two classes of reaction routes to methanol have been debated in literature. One is the formate pathway, where the formation of intermediate HCOO is usually considered to be the rate-determining step.^{208–211} On Cu, the intermediate is a bidentate formate, the most stable adsorbed species; while on ZnO, the intermediate is a monodentate formate.^{212,213} The other pathway involves the formation of CO through the RWGS reaction and the conventional syngas-to-methanol conversion (CO + 2H₂ → CH₃OH).^{96,214} The formate mechanism suggests that CO may be formed from methanol decomposition, while the RWGS mechanism can explain straightforwardly the formation of CO as the major byproduct.^{177,215}

A detailed study was carried out to identify the intermediates for methanol synthesis over Pd/β-Ga₂O₃ using *in situ* FTIR spectroscopy.²¹⁶ The reaction follows the formate pathway, which proceeds through the formation of HCOO, H₂COO (dioxomethylene), CH₃O (methoxy), and the final product, CH₃OH (Scheme 8). The outstanding activity and selectivity of Pd/β-Ga₂O₃ catalyst are attributed to the efficient spillover of atomic hydrogen from Pd surface to the carbonaceous species and the moderate stability of methoxy species on Ga₂O₃. DFT calculations on Cu(111) and Cu₂₉ nanoparticles indicated that the rate-determining steps are



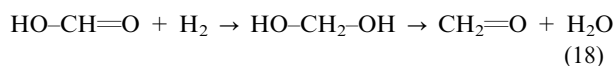
Scheme 8 Reaction pathways for the methanol synthesis from CO₂/H₂ over a palladium/gallia catalyst.

both HCOO and H₂COO hydrogenation.²¹⁷ Compared to Cu(111), the superior activity of Cu nanoparticles for the synthesis of methanol is associated with the active corner sites and structural flexibility, which stabilize the key intermediates (HCOO, H₂COO, and CH₂O) and reduce the barrier of the rate-determining steps.

Based on DFT calculations, Liu *et al.* agreed with the RWGS mechanism by converting CO₂ to CO *via* the HOCO intermediate (Scheme 9) over a molybdenum sulfide (Mo₆S₈) cluster.²¹⁸ The formed CO is then hydrogenated to HCO radical and subsequently methanol. The rate-determining step for the overall reaction is CO hydrogenation to HCO. Mo chemisorbs CO₂, CO, and CH_xO, whereas S facilitates the H–H bond cleavage of molecular hydrogen.²¹⁸

Using kinetic Monte Carlo simulation and DFT calculations, Liu *et al.* found that methanol was produced from both the formate and RWGS routes on Cu/ZrO₂($\bar{1}11$) and Cu/ZrO₂($\bar{2}12$).²⁰⁷ The catalytic activity and selectivity are closely related to the binding strength of atomic oxygen. Thus, optimization of the interfacial property by controlling the oxygen-affinity of the oxide cationic site (*e.g.*, acidity) could enhance CO₂ conversion and selectivity of methanol.

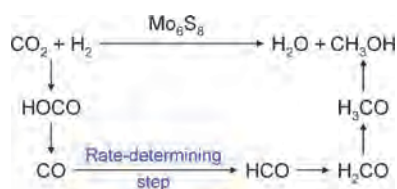
Different from formate or RWGS mechanism, Chan *et al.* systematically studied three-steps hydrogenation of CO₂ to methanol on zeolites (*e.g.*, HZSM-5, ZSM-5) with *ab initio* molecular orbital theory and DFT calculations.^{219,220}



Zeolite-catalyzed hydrogenation reactions are typically sensitive to basicity of the adjacent X group in catalyst and acidity of Brønsted acid (XH) moiety or the nature of metal cation (M) in alkali metal (XM) moiety. The reactivity of an alkali-metal-modified zeolite is enhanced when X becomes more basic. It has been proposed that the zeolites with Ge and N incorporated into the framework would represent effective catalytic activity for hydrogenation processes.²²⁰

6. Synthesis of dimethyl ether

Dimethyl ether is a potential substitute for diesel oil owing to its better combustion performances (*i.e.*, high cetane number, low emissions of NO_x, and near-zero smoke).²²¹ There are two routes for the production of DME from CO₂ hydrogenation—a two-step process (methanol synthesis on a metallic catalyst and subsequent dehydration of methanol on an acid catalyst)



Scheme 9 Possible reaction pathways for synthesis of methanol from CO₂/H₂ on Mo₆S₈.

and a single-step process using a bifunctional catalyst to perform the two steps simultaneously.^{222–226} The main merit of the single-step process on a bifunctional catalyst is the lower thermodynamic limitation than methanol synthesis.

6.1 Hybrid-oxide-based catalysts

The first step in DME synthesis is methanol synthesis in which a Cu-based catalyst is commonly used. The subsequent step is the dehydration of methanol for DME synthesis, which is catalyzed by acidic catalysts such as γ -Al₂O₃, HZSM-5, and NaHZSM-5.¹ Representative catalytic systems for the synthesis of DME are summarized in Table 3.

Selection of acidic support is particularly noteworthy. Jun *et al.* claimed that NaY, which populates with weak acid sites, was inferior in producing DME.²³³ Nevertheless, CuNaY is an excellent dehydration catalyst attributed to the presence of a considerable number of acid sites with moderate strength. In contrast to CO hydrogenation, more water is produced in CO₂ hydrogenation from the RWGS reaction and methanol synthesis. However, formed water decreased the activity of γ -Al₂O₃ due to the high adsorption capacity of water on acid sites.²³⁴ Since HZSM-5 zeolite is not sensitive to the concentration of water, it could be chosen as the composition of the bifunctional catalyst.^{227–229,235,236} Notably, HZSM-5 zeolite is also active for the transformation of DME into hydrocarbons (with ethane and propylene as primary products), even at high Si/Al ratios.²³⁷ These hydrocarbons partially evolve to coke that could block pores of zeolite causing deactivation. A suitable concentration of Na moderates the number and strength of Brønsted acid sites in HZSM-5 zeolite, and prevents the formation of hydrocarbons from DME.^{230,238} For Cu–Zn–Al/NaHZSM-5 catalysts, there is no irreversible deactivation observed.²³⁴ The catalysts can be used uninterruptedly as long as the reaction temperature is well controlled below 300 °C in order to avoid the sintering of CuO nanoparticles.²³⁴

Addition of promoters to Cu-based catalysts leads to an increase in yield of DME. For example, the addition of Ga₂O₃ and Cr₂O₃ increases DME selectivity significantly over a Cu/ZnO catalyst.²³³ Qi *et al.* found that a small amount of MoO₃ addition can enhance the catalytic activity.²³¹ The presence of Mo not only produces new adsorption sites but also enhances binding of adsorbate on the catalyst surface. To increase catalytic reactivity of DME synthesis at low temperature, palladium is added to Cu–Zn–Al–Zr/HZSM-5 catalysts.²³² The addition of Pd markedly boosts DME production and retards CO formation, probably due to the spillover of hydrogen from Pd⁰ to the neighboring phase.²³²

6.2 Theoretical studies

A kinetic model has been proposed for the synthesis of DME in a single reaction step on Cu–Zn–Al/ γ -Al₂O₃ bifunctional catalysts.²²³ The kinetic parameters have been calculated involving the synthesis of methanol, dehydration of DME, and hydrocarbons formation. The kinetic model suitably fits the experimental results obtained in an isothermal fixed bed reactor within a wide range of operating conditions. The model contemplates the role of water in the reaction system,

Table 3 Catalytic systems for the synthesis of DME by hydrogenation of CO₂

Catalysts	T/°C	CO ₂ conversion (%)	DME yield (%)	Ref.
Cu/Zn/Al+HZSM-5	250	n/a	12.5	227
Cu/Ti/Zr+HZSM-5	250	15.6	7.4	228
Cu/Zn/Al/Zr+HZSM-5	250	30.9	21.2	229
Cu/Zn/Al+NaHZSM-5	275	35	26	230
Cu/Mo+HZSM-5	240	12.3	9.5	231
Pd/Cu/Zn/Al/Zr+HZSM-5	200	18.6	13.7	232

n/a: not available.

given that it acts as an inhibitor in the steps of methanol and hydrocarbons synthesis.²²³

Although most researchers believed that DME synthesis is determined by the kinetics rather than thermodynamics, a comprehensive thermodynamic analysis on this process is essential to better understand the intrinsic characteristics.^{239,240}

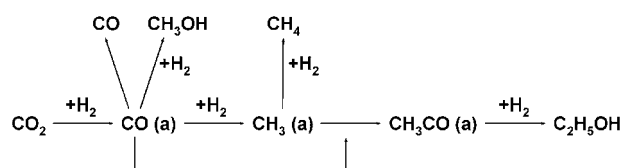
Detailed results of thermodynamic calculations are presented in terms of the equilibrium conversions of CO₂ for DME synthesis.^{241,242} For any feed composition, the equilibrium yields of DME increase with higher pressures but decrease with higher temperatures.

7. Synthesis of higher alcohols

Higher alcohols are preferable to methanol as products of CO₂ hydrogenation from viewpoint of safe transport and excellent compatibility to gasoline.¹⁶ Direct synthesis of higher alcohols from CO₂ could be regarded as a combination of the RWGS reaction and subsequent the formation of higher alcohols from syngas.¹⁶ Hence, a catalyst that is active for both reactions under the similar condition would be favorable for the overall reaction, for example, Fe-based and Rh-based catalysts.^{243–249}

Catalysts for the formation of ethanol require active centers for promoting partial reduction of CO₂ to CO, C–C bond formation, and OH group insertion.^{247,249} Fe-based FT catalysts mixed with Cu-based catalysts have the functions of partial reduction of CO₂ to CO and ethanol synthesis.^{247,249} Addition of small concentrations of Pd and Ga can maintain the optimal redox state during the reaction, and promote the formation of ethanol. Further improvement has been expected by combination of basic compounds, such as potassium carbonate, with the polyfunctional composite catalyst leading to the suppressed formation of methane.²⁴⁹ For example, Arakawa *et al.* reported that doping K₂CO₃ on a Cu/Fe/ZnO catalyst increased the selectivity of ethanol from ~6% to ~20% at 300 °C and 7 MPa.^{250,251}

An alternative route for improving the yield of ethanol from CO₂ is based on an observation that syngas can be converted into ethanol over Rh/SiO₂ catalyst with methane as another main product.²⁴⁴ However, by adding various metal oxide to the catalysts, CO₂ conversion and selectivity to alcohols could be increased.²⁴⁴ The addition of Li to Rh/SiO₂ yields an ethanol selectivity of 15.5% and a CO₂ conversion of 7.0%. *In situ* FTIR analysis suggests that CO₂ is hydrogenated to ethanol *via* CO intermediate, the amount of which is increased by increasing Li loading.²⁴⁴ A plausible mechanism of ethanol formation is proposed in Scheme 10. With a 5 wt% Rh–Fe/SiO₂ catalyst, a CO₂ conversion of 26.7% and an



Scheme 10 Plausible reaction mechanism of CO₂ hydrogenation to ethanol. Reproduced with permission from ref. 244. Copyright 1996 Elsevier.

ethanol selectivity of 16% were obtained at 260 °C.²⁴⁶ Based on results of XPS and *in situ* FTIR, the authors have concluded that Fe³⁺ changes the electronic states of Rh, and the presence of Fe⁰ promotes methanation and prevents formation of methanol, ethanol, and CO.²⁴⁶

The promoting effect of anionic Se is realized by modifying the electronic states of active sites of Rh/SiO₂ or by the direct coordination of Se to surface intermediate species.^{252,253} Kurakata *et al.* used Rh₁₀Se/TiO₂ catalyst for CO₂ hydrogenation in a closed circulating reaction system at a fairly low pressure, and reported that the selectivity of ethanol could reach as high as 83%.^{243,248} The mechanism proposed for ethanol synthesis on Rh₁₀Se/TiO₂ is depicted in Fig. 6.^{245,248} CH_{x,ads} species on rhodium reacts with CO_{y,ads} to form acetate, which is subsequently hydrogenated to ethanol on Rh sites. The reaction of CO and H₂ proceeds fairly slowly and the products distribution is entirely different from that of CO₂ hydrogenation on Rh₁₀Se/TiO₂ catalyst. The results suggest that ethanol synthesis does not occur *via* CO over the catalyst.²⁴³

Additionally, a multi-step method for using CO₂ *via* the RWGS reaction as a source of CO was introduced by Tominaga *et al.* in hydroformylation reaction.²⁵⁴ Hydroformylation with CO₂ proceeds in two steps—CO₂ is first converted into CO, which further involves in hydroformylation

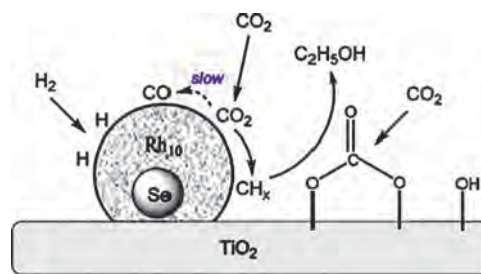
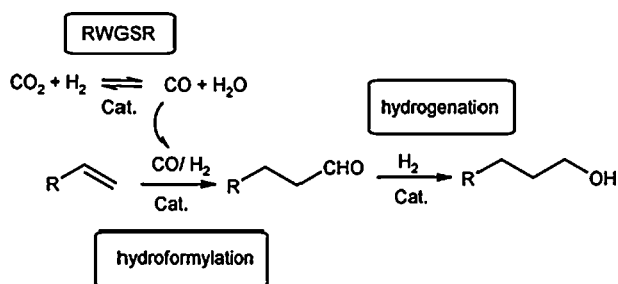


Fig. 6 Proposed mechanism for ethanol synthesis from CO₂ hydrogenation on a Rh₁₀Se/TiO₂ catalyst. Reproduced with permission from ref. 16. Copyright 2009 Elsevier.



Scheme 11 Formation of alcohols from alkenes by hydroformylation with CO₂. Reproduced with permission from ref. 259. Copyright 2009 Elsevier.

of the substrate (Scheme 11). Ruthenium carbonyls, particularly multinuclear ruthenium clusters, are active for the process since they are capable of catalyzing both of steps (*i.e.*, the RWGS reaction and the subsequent hydroformylation).^{254–259} A potential side reaction—hydrogenation of alkene—could be inhibited by adding an alkali metal or alkaline earth halide or by using ionic liquid as the solvent. In the latter case, ionic liquid acts as both promoter and solvent, and the yield of heptanol could reach 82%.²⁵⁸

8. Synthesis of formic acid and formates

Formic acid is widely used in many fields, such as the leather and rubber industries.²⁶⁰ It can also be used as a feedstock for producing numerous chemicals (*e.g.*, fiber, sweetener). Since the beginning of 1990s, there has been an increasing interest in the hydrogenation of CO₂ to formic acid and formates.³¹ Recently, formic acid has been considered as hydrogen storage material by combining CO₂ hydrogenation with selective formic acid decomposition.^{31,261} Hence, improvements with respect to catalyst stability and activity have been continuously accomplished.



To shift the reaction equilibrium, it is necessary to add a base (inorganic or organic) to the reaction system.²⁶⁰ With the

addition of an inorganic base, formate is generated which subsequently needs strong acid to convert to formic acid. For the organic base, recovery of formic acid is complicated and energy consuming due to the volatility of the base.²⁶⁰

8.1 Active homogeneous catalysts

Compared to heterogeneous systems for CO₂ hydrogenation, the formation of formic acid and formates typically proceeds with organometallic complexes at low temperatures.³¹ Table 4 summarizes representative transition-metal catalysts based on rhodium, ruthenium, and iridium for hydrogenation of CO₂ to formic acid and formates.^{14,15,31}

We need to mention the Wilkinson catalyst, RhCl(PPh₃)₃, which was first introduced by Inoue *et al.* in 1976 for CO₂ hydrogenation.²⁷⁶ The use of this complex has been studied in more details by Ezhova *et al.* who found that formic acid was formed in the presence of rhodium complexes with a phosphine ligand.²⁶² The activity of the catalyst is strongly dependent on the nature of solvent, giving high rates in polar solvents (*e.g.*, DMSO and MeOH). The beginning and end of CO₂ hydrogenation is coincided with the appearance and disappearance of RhCl(PPh₃)₂(NET₃), respectively, which is a precursor of the catalytically active complex. Reduction of the complex to metallic Rh is inhibited by excess PPh₃, which increases the yield of formic acid significantly.

Ru complexes generally offer favorable activity and selectivity for formic acid, and have become focus of studies.²⁶³ Tai *et al.* compared the effectiveness of Ru(II) catalysts with various phosphines or other ligands through *in situ* catalyst formation.²⁷⁷ There is no correlation found between the basicity of monophosphines (PR₃) and the activity of the catalysts. Among the diphosphines, a rather unusual interplay of electronic and bite angle effects was observed (Fig. 7). Weakly basic diphosphines (bis(diphenylphosphino) compounds) form highly active catalysts only if their bite angles are small, while more strongly basic diphosphines (bis(dicyclohexylphosphino) compounds) show the opposite trend. Ru/Mo heterobimetallic complex exhibits low activity for CO₂ hydrogenation, attributing to the non-facile reaction of the complex with H₂ to yield the active dihydride species.²⁶⁴

Table 4 Catalytic hydrogenation of CO₂ to formic acid and formates

Catalyst precursor	Solvent	Additives	$p(\text{H}_2)/p(\text{CO}_2)$ (atm)	$T/^\circ\text{C}$	TON ^c	TOF (h ⁻¹)	Ref.
RhCl(PPh ₃) ₃	MeOH	PPh ₃ , NEt ₃	20/40	25	2700	125	262
Ru ₂ (CO) ₅ (dppm) ₂ ^a	acetone	NEt ₃	38/38	RT ^c	207	207	263
CpRu(CO)(μ-dppm)Mo(CO) ₂ Cp ^a	C ₆ H ₆	NEt ₃	30/30	120	43	1	264
TpRu(PPh ₃) ₃ (CH ₃ CN)H ^a	THF ^b	NEt ₃ , H ₂ O	25/25	100	760	48	265
TpRu(PPh ₃) ₃ (CH ₃ CN)H ^a	CF ₃ CH ₂ OH	NEt ₃	25/25	100	1815	113	266
RuCl ₂ (PMe ₃) ₄	scCO ₂	NEt ₃ , H ₂ O	80/140	50	7200	153	267
RuCl(OAc)(PMe ₃) ₄	scCO ₂	NEt ₃ /C ₆ F ₅ OH	70/120	50	31 667	95 000	268
(η ⁶ -arene)Ru(oxinato)	H ₂ O	NEt ₃	49/49	100	400	40	269
(η ⁶ -arene)Ru(bis-NHC) ^a	H ₂ O	KOH	20/20	200	23 000	306	270
[Cp*Ir(phen)Cl]Cl	H ₂ O	KOH	29/29	120	222 000	33 000	271
PNP-Ir(III)	H ₂ O	KOH, THF ^b	29/29	120	3 500 000	73 000	272
Cp*Ir(NHC)	H ₂ O	KOH	30/30	80	1600	88	273
NiCl ₂ (dcpe) ^a	DMSO ^b	DBU ^b	40/160	50	4400	20	274
Si-(CH ₂) ₃ NH(CSCH ₃)-Ru	C ₂ H ₅ OH	PPh ₃ , NEt ₃	39/117	80	1384	1384	275
Si-(CH ₂) ₃ NH(CSCH ₃)-{RuCl ₃ (PPh ₃)}	H ₂ O	IL	88/88	80	1840	920	260

^a dppm = Ph₂PCH₂PPh₂; Tp = hydrotris(pyrazolyl)borate; NHC = N-heterocyclic carbene; dcpe = Cy₂PCH₂CH₂PCy₂; THF = tetrahydrofuran.

^b DMSO = dimethyl sulfoxide; DBU = 1,8-diazabicyclo[5.4.0]undec-7-ene. ^c RT = room temperature; TON = turnover number.

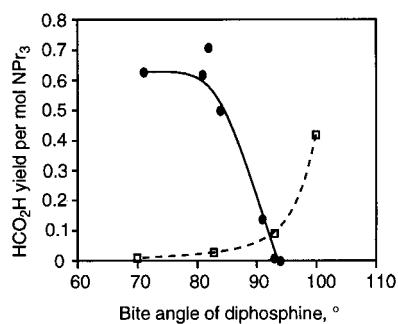


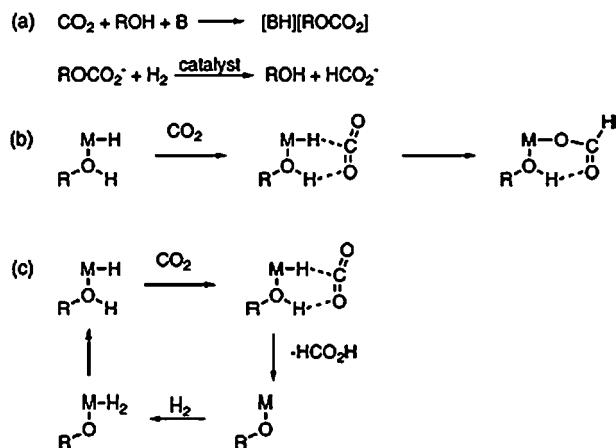
Fig. 7 Dependence of the yield of formic acid in the first 1 h on the bite angle of the diphosphines, showing bis(diphenylphosphino) compounds (●) and bis(dicyclohexylphosphino) compounds (□). Reproduced with permission from ref. 277. Copyright 2002 American Chemical Society.

Addition of a small amount of water is efficient to improve the catalytic hydrogenation of CO₂ to formic acid.^{267,274,278}

It was supposed that hydrogen-bonding interaction between H₂O molecule and an oxygen atom of CO₂ enhanced the electrophilicity of carbon and facilitated its insertion into the metal-hydride bond.^{265,278} According to high pressure nuclear magnetic resonance (NMR) data and theoretical calculations, Yin *et al.* proposed a reaction mechanism to account for the “water effect” using the ruthenium complex TpRu(PPh₃)(CH₃CN)H.²⁶⁵ The key intermediate in the catalytic cycle is an aquo metal hydride species, TpRu(PPh₃)(H₂O)H, formed by a ligand displacement reaction of H₂O. The intermediate transfers a hydride and a proton simultaneously to CO₂ to yield formic acid and itself is converted to a transient hydroxo species, which then associates a H₂ molecule to regenerate TpRu(PPh₃)(H₂O)H. The same group subsequently studied the effect of alcohol on the same catalyst.²⁶⁶ The key species of the catalytic process, TpRu(PPh₃)(ROH)H, is the alcohol analogue of the aquo hydride complex. Among the alcohols, pronounced promoting effect of CF₃CH₂OH is resulted from the enhanced electrophilicity of the carbon atom of CO₂, which is due to the strong interaction between an oxygen atom of CO₂ and the highly acidic hydrogen in the intermediate.

Munshi *et al.* described a detailed study regarding the effect of bases and alcohols on hydrogenation mechanism.²⁶⁸ Use of DBU rather than NEt₃ increases the rate of reaction by an order of magnitude owing to the ability of DBU in trapping CO₂.^{279,280} Based on *in situ* NMR spectroscopy, alcohol induces the Ru-based precursor to transform into a cationic complex.²⁶⁸ The alcohol is not likely to generate carbonic acids or protonated amines in solution (Scheme 12(a)), but could either help insert CO₂ into the M–H bond (Scheme 12(b)) or hydrogenate CO₂ in a concerted ionic hydrogenation mechanism (Scheme 12(c)).

Hydrogenation of scCO₂ has gained a growing interest since CO₂ can play a dual role as both reactant and solvent.⁶ High rates of hydrogenation were obtained by Jessop *et al.* using soluble RuXY(PMe₃)₄ catalysts (X, Y = H, Cl, or O₂CMe) in a scCO₂ solution, which can be ascribed to several factors, including easy separation, improved mass- and heat-transfer properties, and high solubility of H₂ with scCO₂.^{267,281,282}

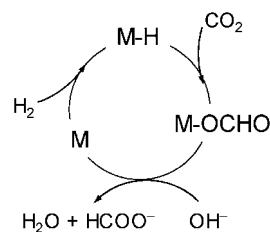


Scheme 12 Three possible explanations for involvement of alcohol in the CO₂ hydrogenation. Reproduced with permission from ref. 15. Copyright 2004 Elsevier.

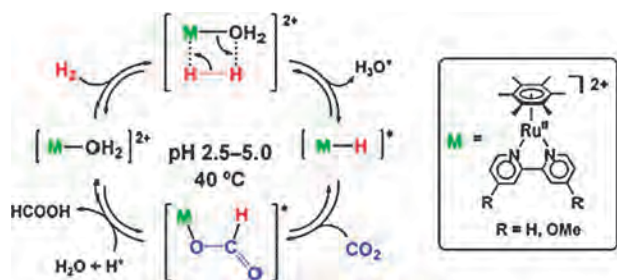
Results of kinetic studies exhibited that the reaction of scCO₂ hydrogenation is in first order under experimental conditions.²⁸² The rate is strongly dependent on the choice of additive.

Water can also be employed as the solvent for the synthesis of formic acid, especially for formate formation. As an inexpensive, abundant, and innocuous solvent, water offers certain advantages such as amphoteric behavior in Brønsted sites, high absorption for some gases, and easy separation from apolar compounds.²⁸³ On the other hand, catalysis in water requires water-soluble ligands for the catalysts. A series of Ir and Ru complexes have been exploited for CO₂ hydrogenation to formic acid or formate in alkaline aqueous solution.^{269–273,283,284} The catalysts containing the stronger electron donor ligands could accelerate the reaction.^{270,283} Ir complex prepared by Himeda *et al.* is homogeneous and highly reactive at the beginning of the reaction; however, it turns into heterogeneous and deactivates at the end of the reaction.^{271,283,284} The solvent, product, and catalyst could be easily separated by conventional filtration and evaporation without generation of waste. A plausible mechanism has been discussed where a catalytic cycle for CO₂ hydrogenation by Ir or Ru complexes involves a hydrido complex formed *in situ* from the corresponding aqua or chloro complexes (Scheme 13).^{269,271,272} CO₂ inserts into the hydrido complex to give the corresponding formyl complex, which then reacts with hydroxide to produce the formate anion.

Hydrogenation of CO₂ into formic acid under acidic conditions (pH of 2.5–5.0) without any base in water has been achieved by using water-soluble ruthenium aqua complexes,



Scheme 13 Plausible reaction scheme for hydrogenation of CO₂ using Ir or Ru complexes.



Scheme 14 Plausible reaction scheme for aqueous hydrogenation of CO₂ under acidic conditions. Reproduced with permission from ref. 285. Copyright 2004 Royal Society of Chemistry.

with TON of 55 after 70 h at 40 °C.²⁸⁵ The hydride species generated by the reaction of the aqua complex with H₂ at pH of 2.5–5.0 reacts with CO₂ to afford the formate complex (Scheme 14).

There is limited work on exploring active components containing metals from non-platinum groups. Tai *et al.* found that combinations of FeCl₃, NiCl₂, or MoCl₃ with dpep yielded significant activity for CO₂ hydrogenation to formic acid.²⁷⁴ Merz *et al.* reported the remarkably distinct reactivity of hydrido zinc heterobimetallic cubanes towards CO₂ hydrogenation.²⁸⁶ The hydride transfer from Zn–H to CO₂ is substantially accelerated in the presence of Li ions leading to the respective metal formate hydrates.

Formic acid esters can be formed by the hydrogenation of CO₂ in alcohol solvents.²⁸⁷ Methyl formate (MF) was synthesized efficiently by hydrogenation of scCO₂ in methanol solvent over a ruthenium catalyst with TOF of 55 h⁻¹ in 80 °C.^{267,288} Formic acid is formed initially and subsequently reacts with methanol to produce MF. Yu *et al.* demonstrated a one-step CO₂ hydrogenation to MF over a Pd/Cu/ZnO catalyst with excessive methanol in hydrogen.²⁸⁹ During the reaction, CO₂ can be activated as methyl formate with high yield (>20%) and excellent selectivity (>96%). Doping the material with noble metals (such as Pd, Ru, and Au) greatly influences TOF, and Pd has been proved to be the best modifier.²⁸⁹ This trend may be related to the ability of the hydrogen activation and transfer of the promoter on the catalyst surface since Pd exhibits the best hydrogen spillover activity among the noble metals.²⁹⁰ Au yields low TOF, which could be related to its high affinity for Cu (*e.g.*, lattice match and alloy formation), blocking surface sites. To increase reactivity of MF from CO₂ hydrogenation, one must break the equilibrium limit by either replacing the batch process with a continuous process or removing the products promptly.²⁹⁰

8.2 Synthesis of formic acid by immobilized ruthenium catalysts

Although homogeneous catalysts have been proved to be efficient for CO₂ hydrogenation to formic acid, they have some drawbacks such as separation of products and recycling the catalyst. Immobilization of a complex onto a supporting material would improve the reusability and stability of the catalyst. Ruthenium complexes immobilized over amine-functionalized-silica have been developed with an *in situ* synthetic approach for CO₂ hydrogenation to formic acid.²⁷⁵ The catalyst not only exhibits high activity and 100% selectivity, but also offers the practical advantages such as easy separation and recycling.²⁷⁵

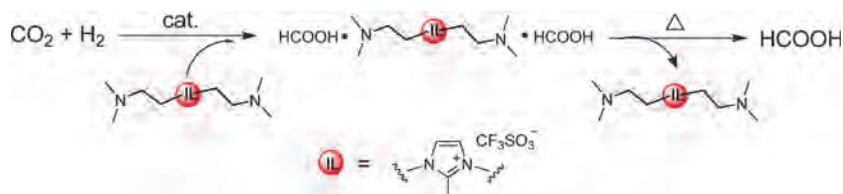
Ionic liquids have some unique properties, such as excellent thermal stability, wide liquid regions, and favorable solvation properties for various substances.²⁶⁰ Zhang *et al.* reported that the combination of a basic ionic liquid and a silica-supported ruthenium complex promoted CO₂ hydrogenation to formic acid with satisfactory activity and selectivity (Scheme 15).^{260,291} Upon the reaction, formic acid could be collected by heating due to the non-volatility and moderate basicity of ionic liquid.

8.3 Mechanistic understanding

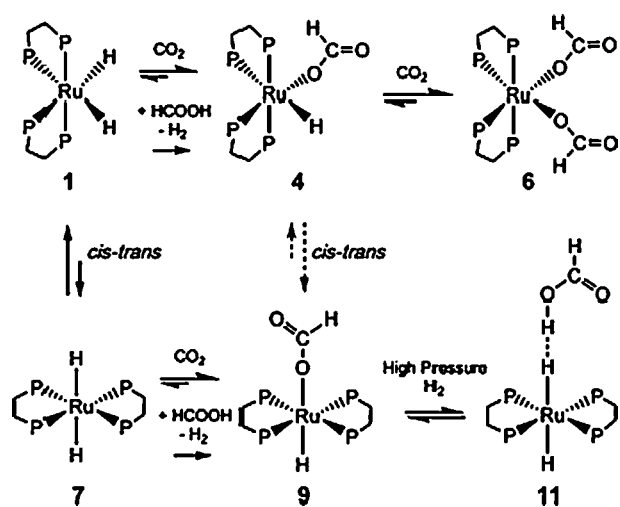
There have been arguments for years between the theoretical understanding and experimental observation for the synthesis of formic acid. For example, from a theoretical point of view, the rate-determining step is CO₂ insertion into a ruthenium hydride complex, which, in contrast, is a facile step in experimental studies.^{292–295}

Musashi and Sakaki presented a mechanistic investigation regarding the rhodium(III)-catalyzed CO₂ hydrogenation to formic acid.²⁹⁶ The first step of the reaction is the insertion of CO₂ into the Rh(III)–H bond of the active species [RhH₂(PH₃)₂(H₂O)]⁺. There are two possible subsequent reaction routes. One involves a sequence of oxidative and reductive elimination steps for the hydrogen activation pathway upon the insertion of CO₂.²⁹⁷ In the other pathway, formation of formic acid was observed upon addition of hydrogen to the rhodium formate intermediate obtained from CO₂ insertion.²⁹⁸ In both reaction routes, the rate-determining step is CO₂ insertion into the Rh(III)–H bond.²⁹⁶

Complete reaction pathways relevant to CO₂ hydrogenation using homogeneous ruthenium dihydride catalysts (Scheme 16) have been investigated by experimental and theoretical study.^{295,299} Simulations indicate that CO₂ insertion, which leads to the formation of formate complexes, is a rapid process with a relatively low activation barrier.



Scheme 15 Reaction scheme and separation process for the hydrogenation of CO₂ promoted by [DAMI][TfO]. Reproduced with permission from ref. 260. Copyright 2009 Wiley-VCH Verlag GmbH & Co.

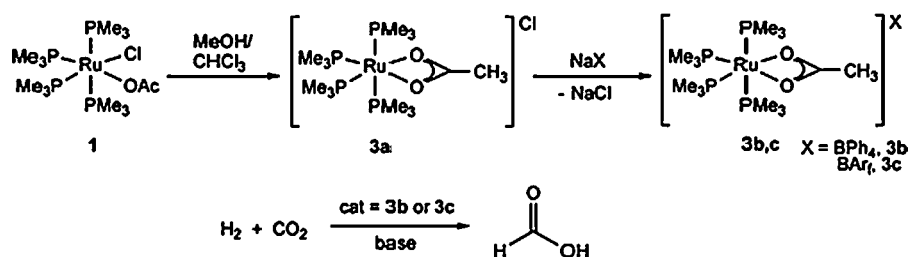


Scheme 16 Reaction pathways of CO₂ hydrogenation using a ruthenium dihydride catalyst. Reproduced with permission from ref. 296. Copyright 2007 Wiley-VCH Verlag GmbH & Co. KGaA.

Subsequent H₂ insertion into the formate-Ru complex, which is the rate-determining step, occurs *via* an intermediate [Ru(η²-H₂)] complex following formic acid.²⁹⁹ The activation energy of the H₂ insertion step is lower for the *trans* isomer than that for the *cis* isomer.²⁹⁹

Complex *cis*-(PMe₃)₄RuCl(OAc) (**1**, OAc is acetate) has performed favorable activity for CO₂ hydrogenation as shown in Table 4.²⁶⁸ High pressure NMR spectroscopy was employed to investigate the mechanism of formic acid synthesis catalyzed by complex **1** and its derivatives **3b** and **3c** (Scheme 17).³⁰⁰ Complexes **3b** and **3c** are as efficient as **1** in the presence of an alcohol cocatalyst. An unsaturated, cationic ruthenium complex [(PMe₃)₄RuH]⁺ (denoted as **B**) has been proposed as an active component for the reaction. The base in the system not only traps formed formic acid but also involves in the conversion of **3b** and **3c** to **B**.³⁰⁰

Following the work presented by Nozaki *et al.* (Scheme 13), Ahlquist studied, in a detailed manner, the mechanism of a model Ir(III) catalyst reacting with CO₂ and H₂ under basic conditions employing DFT calculations.^{272,301} The author found that the formation of formate complex proceeded *via* a two-step mechanism. The rate-determining step is the regeneration of the Ir(III) trihydride intermediate, which agrees with the experimental results that stronger basicity leads to higher conversion rates.³⁰¹ The formation of the iridium trihydride proceeds *via* formation of a cationic Ir(H)₂(H₂)



Scheme 17 Mechanism of CO₂ hydrogenation into formic acid *via* complex **1** and its derivatives. Reproduced with permission from ref. 301. Copyright 2009 American Chemical Society.

complex, where the base abstracts a proton from the dihydrogen ligand.³⁰¹

To provide theoretical answers to questions regarding why and how water molecules accelerate the reaction, Ohnishi *et al.* theoretically investigated the role of water in Ru(II)-catalyzed hydrogenation of CO₂ into formic acid (Scheme 18).^{294,302} The active species are *cis*-Ru(H)₂(PMe₃)₃ and *cis*-Ru(H)₂(PMe₃)₃(H₂)₂ with and without water, respectively. In the absence of water molecules, the Ru(η¹-formate) intermediate is produced through CO₂ insertion, whereas the existence of water molecules facilitates nucleophilic attack of the H ligand to CO₂, which accounts for acceleration of the reaction.³⁰² The metathesis is the rate-determining step in the presence of water molecules. The activation barrier of this process is much lower than that of CO₂ insertion into the Ru–H bond.³⁰² Notably, both alcohols and amines can accelerate the nucleophilic attack in the same manner as water.³⁰²

As mentioned in section 8.1, ruthenium or iridium aquo complexes could catalyze CO₂ hydrogenation to formic acid without the addition of any base at pH of 3.0 in H₂O.^{285,303} Both of Ru and Ir complexes share the similar mechanism (Scheme 19), but differ in the nature regarding the rate-determining step. The rate-determining step for the hydrogenation with the ruthenium catalysts is the reaction of the aquo complex with H₂, whereas for the iridium catalysts the rate-determining step is the reaction between the hydride complex and CO₂.³⁰³

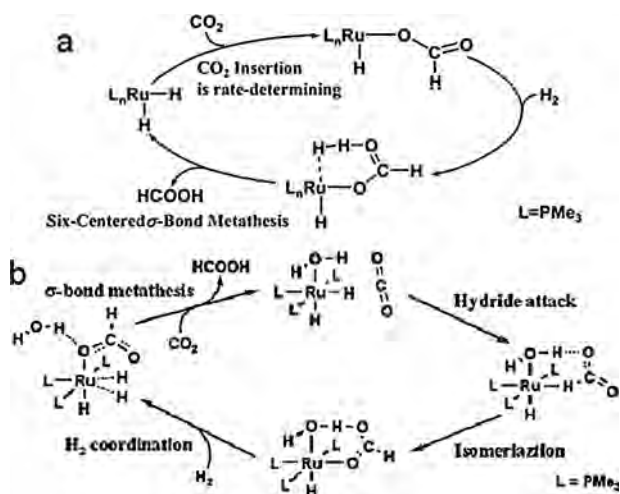
9. Synthesis of formamides

A step toward green formylation of amines is the use of CO₂ and H₂ as formylation agents instead of toxic compounds such as CO and phosgene.

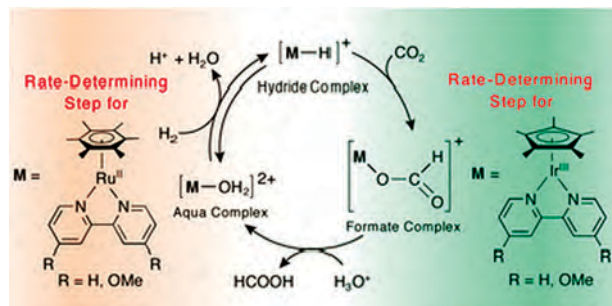


Similar to the formation of formic acid, scCO₂ has also been applied successfully to the synthesis of formamides. Particularly, conversion of CO₂, H₂, and secondary amines to the corresponding formamides with ruthenium complexes has gained increasing attention. We list typical catalytic systems for formylation of amines with CO₂ in Table 5.^{14,29}

Synthesis of *N,N*-dimethylformamide (DMF) from CO₂, H₂, and dimethylamine has been examined by several groups. Jessop *et al.* pioneered the field and reported a high TOF up to 10 000 h⁻¹ using RuCl₂[P(CH₃)₃]₄.³⁰⁴ The reaction proceeds with two steps—CO₂ hydrogenation to the formate compound



Scheme 18 Mechanism of Ru(II)-catalyzed hydrogenation of CO₂ into formic acid in the absence (a) or presence (b) of water molecules. Reproduced with permission from ref. 295 and 303. Copyright 2005 and 2006 American Chemical Society, respectively.



Scheme 19 Mechanisms of CO₂ hydrogenation by Ru(II) and Ir(III) aqua complexes under acidic conditions. Reproduced with permission from ref. 304. Copyright 2006 Royal Society of Chemistry.

followed by dehydration to formamide. Reaction mixture typically consists of a homogeneous supercritical phase and an insoluble carbamate liquid (Fig. 8). Under the relatively drastic reaction conditions (100 °C, 210 atm), the formation of DMF takes place in liquid phase and mostly dissolves in the

supercritical phase.³⁰⁴ Meanwhile, the water content in the liquid phase is increased because of its low solubility in scCO₂. Krocher's group discovered that RuCl₂(dppe)₂ was even more active than RuCl₂[P(CH₃)₃]₄ for the catalytic synthesis of DMF with TOF as high as 360 000 h⁻¹.²⁸⁷

Although scCO₂ is an advantageous reaction medium, the rate of DMF formation may drastically drop as a result of the subtle phase behavior during the reaction. The co-product (*i.e.*, water) can be precipitated in the scCO₂ phase, which results in the phase separation between the catalyst and dimethylamine. The use of water-soluble catalyst (*e.g.*, Ru-P(CH₂OH)₃) could combine effectively with the reaction mixture including the scCO₂ and co-product water.³⁰⁹ Kayaki *et al.* synthesized a series of water-soluble Ru complexes by ligand substitution, which yielded TONs ranged from 2100 to 4800.³¹⁰

Heterogenization of Ru(II) complex over an insoluble substrate for the DMF synthesis is a relatively new direction in the field. Baiker *et al.* found that sol-gel, silica- and aerogel-supported analogues of RuCl₂(dppm)₂, RuCl₂(dppp)₂, RuCl₂[P(CH₃)₃]₄, and related complexes had both recyclability and considerable TOF values.^{305,306,311,312} The structures of these hybrid materials affect the outcome of DMF synthesis, indicating that a suitable choice of supporting material for immobilization of the Ru complexes is fairly important. Ikariya's group prepared Ru-based catalysts supported on a cross-linked graft copolymer resin.³¹³ The catalysts not only exhibit hydrophilic property but are also recyclable.

Synthesis of higher formamides has also been performed by a number of groups. Liu *et al.* showed that the RuCl₂(dppe)₂ catalyst could be employed in an ionic liquid ([BMIM][PF₆]) for the synthesis of di-*n*-propylformamide from CO₂, H₂, and di-*n*-propylamine.³⁰⁷ The product could be extracted from the ionic liquid, and both the catalyst and ionic liquid can be recycled. The reaction system containing scCO₂ and ionic liquid may offer particular advantages as a new biphasic catalysis process. Formylation of various cyclic and aliphatic amines with scCO₂ using the ruthenium catalyst RuCl₂(dppe)₂ affords almost 100% selectivity.^{314,315} A complex phase behavior of the reaction mixture was observed during the reaction, including formation of solid carbamate.³¹⁴

Table 5 Catalytic systems for the synthesis of formamides by the hydrogenation of CO₂

Catalyst	Solvent	Additive	T/°C	Yield (%)	TON	TOF (h ⁻¹)	Ref.
RuCl ₂ [P(CH ₃) ₃] ₄	scCO ₂	NH(CH ₃) ₂	100	76	370 000	10 000	304
RuCl ₂ [P(CH ₃) ₃] ₄	scCO ₂	NH(CH ₃) ₂	100	n/a	420 000	6000	267
RhClX ₃ ^a	scCO ₂	NH(CH ₃) ₂	100	4	530	35	305
IrClX ₃ ^a	scCO ₂	NH(CH ₃) ₂	100	23	2900	190	305
PdCl ₂ X ₃ ^a	scCO ₂	NH(CH ₃) ₂	100	11	1410	90	305
PtCl ₂ X ₃ ^a	scCO ₂	NH(CH ₃) ₂	100	10	1490	100	305
RuCl ₂ X ₃ ^a	scCO ₂	NH(CH ₃) ₂	100	35	4420	290	305
RuCl ₂ Z ₃ ^a	scCO ₂	NH(CH ₃) ₂	133	82	110 800	1860	305
RuCl ₂ (dppe) ₂ ^a		NH(CH ₃) ₂	100	n/a	740 000	360 000	287
RuCl ₂ (dppp) ₃ ^a		NH(CH ₃) ₂	110	n/a	n/a	18 400	306
RuCl ₂ [P(CH ₃) ₃] ₄	scCO ₂	NH(C ₂ H ₅) ₂	100	n/a	820	63	267
RuCl ₂ [P(CH ₃) ₃] ₄	scCO ₂	NH ₂ (<i>n</i> -C ₃ H ₇)	100	n/a	260	52	267
RuCl ₂ (dppe) ₂ ^a	scCO ₂ /IL	NH(<i>n</i> -C ₃ H ₇) ₂	80	99	110	22	307
Cu/ZnO		NH(CH ₃) ₂	140	97	n/a	n/a	308

^a X = PPPh₂(CH₂)₂Si(OEt)₃; Z = PMe₂(CH₂)₂Si(OEt)₃; dppe = Ph₂P(CH₂)₂PPh₂; dppp = Ph₂P(CH₂)₃PPh₂. n/a: not available.

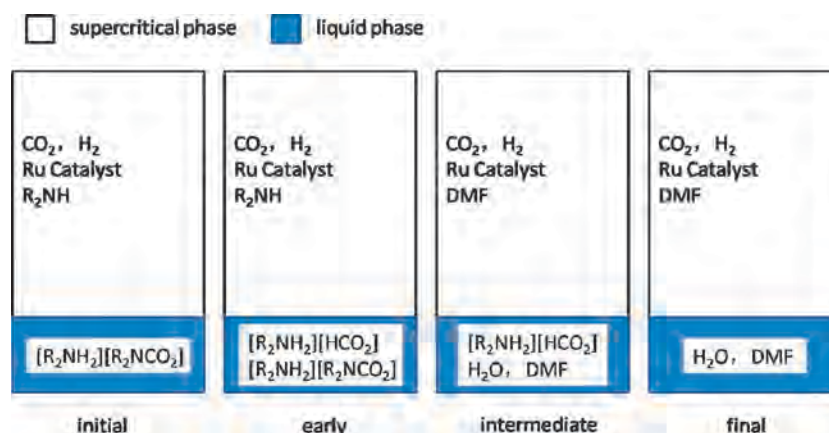
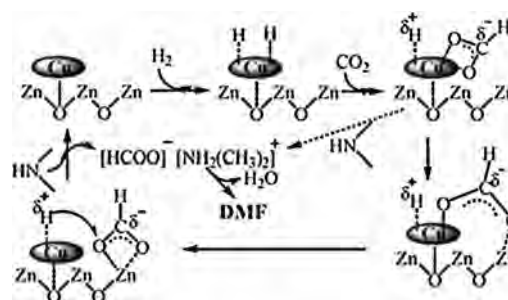


Fig. 8 The composition of the phases during the reaction. Reproduced with permission from ref. 305. Copyright 1994 American Chemical Society.

Addition of water to the reaction mixture suppresses formation of the carbamate and enhances the rate of reaction.³¹⁵ Additionally, Jessop's group, for the first time, prepared formamide from CO₂, H₂, and aniline with a RuCl₂[P(CH₃)₃]₄ catalyst.³¹⁶ We should note that the basicity of aniline is not strong enough to promote the hydrogenation of CO₂ to formate salt, which is the first step for formamide synthesis.¹⁵ However, addition of a stoichiometric amount of DBU yields excellent selectivity with a yield of 72% for formamide.

Due to the complicated procedures for preparing Ru complexes, more easily accessible processes have been explored. A simple route for preparing highly active and selective ruthenium based catalysts was carried *in situ* from RuCl₃ or Ru/Al₂O₃ in the presence of phosphine, dppe or PPh₃ (Scheme 20).^{317,318} Catalytic performances of *in situ* generated homogeneous catalysts lead to high activity and 100% selectivity. The structure and activity of the formed catalysts are similar to those of the RuCl₂(dppe)₂ and RuCl₂(PPh₃)₃. The utilization of this simple method for catalyst preparation offers an economical and green formylation process with high activity and selectivity.

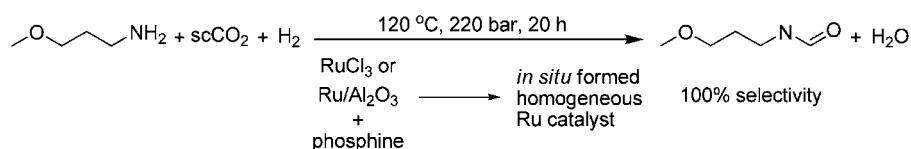
In addition to Ru-based catalysts, Liu *et al.* found a synergistic effect over Cu/ZnO catalyst for the synthesis of DMF in solvent-free conditions.³⁰⁸ A tentative reaction mechanism is proposed in Scheme 21. Hydrogen is first activated on the surface of copper and subsequently forms formate species with CO₂. DMF is generated by two possible routes from formate species. The formate can be directly hydrogenated to formic acid on a Cu surface, and then reacts with dimethylamine to form DMF. Alternatively, formate species and activated hydrogen on Cu surface migrate to the surface of ZnO, and subsequently combine with dimethylamine to form DMF.³¹⁹



Scheme 21 Proposed mechanism for synthesis of DMF from CO₂, H₂, and dimethylamine catalyzed by Cu/ZnO. Reproduced with permission from ref. 309. Copyright 2010 Royal Society of Chemistry.

10. Concluding remarks and perspectives

As a major greenhouse gas, carbon dioxide with increased concentration in the atmosphere is being considered responsible for the global warming and climate changes. Therefore, the reduction of CO₂ concentration becomes the global focus. Being a renewable and environmentally friendly source of carbon, conversions of CO₂ to fuels and chemicals offer opportunities to mitigate the increasing CO₂ buildup. As discussed in this review, hydrogenation of CO₂ is a feasible and powerful process with this regard. However, one need to recall the nature of CO₂—chemically stable and thermodynamically unfavorable. To eliminate the limitations on the conversion and selectivity, various technical directions and specific research approaches on rational design of catalysts, reactor optimization, and exploration of reaction mechanisms have been presented. In addition to our review on recent advances in the field, it would be even useful to provide a framework for research prospects which would guide the future research direction in the laboratories and industries.



Scheme 20 Formylation of 3-methoxypropylamine with H₂ and sCO₂ over ruthenium catalysts.

Both homogenous and heterogeneous catalysts play crucial roles in the hydrogenation of CO₂. Homogeneous catalysts (e.g., Ru-, Rh-, and Ir-based catalysts) are efficient for the formation of formic acid and formates. The reactions can be accelerated by the addition of solvents such as water, supercritical CO₂, and ionic liquids. However, the need for expensive catalyst, high operating pressure, and the tedious workup procedures involved for catalyst separation and recycling make these processes unattractive for commercial applications. Therefore, researchers have paid increasing attention on the immobilization of homogenous catalysts to combine the efficient activity with the properties of separation and recyclability. Heterogeneous catalysts (e.g., Fe-, Cu-, and Ni-based catalysts) are, of course, more practical for industrial applications compared to homogeneous catalysts. The catalyst with larger surface area, ultrafine particle, and higher metal dispersion can usually possess higher activity and selectivity, and longer life in the hydrogenation of CO₂. However, these heterogeneous catalysts frequently suffer from low yield and poor selectivity due to fast kinetics of the C–H bond formation. Furthermore, preparation methods have considerable influences on the nature of the catalysts (such as BET surface area, particle size, metal dispersion, *etc.*), leading to the disparities of the catalytic performance. Therefore, in order to make CO₂ hydrogenation economically feasible, significant improvements in new catalytic systems with rational design and molecular simulations would be necessary.

Even though a large number of investigations have been done with experimental observations and theoretical analyses, mechanisms of CO₂ hydrogenation are still in dispute. For example, fundamental understanding regarding the role of added solvent at molecular level in the homogeneous systems is unclear. In heterogeneous reaction, the prevalent consensus is that the active site is provided by the synergy between the primary catalyst and the support or the promoter. Nevertheless, the nature of the active sites and interactions among active components, support, and promoter as well as reaction mechanisms are still elusive, even for the synthesis of formic acid, the first step of the hydrogenation. For both homogeneous and heterogeneous catalysts, the primary focus of the mechanisms for CO₂ hydrogenation is on how and where CO₂ is activated and interacts with hydrogen and/or hydroxyl species under different reaction conditions. Surface science approaches coupled with molecular simulations would bridge the gap between the macroscopic characteristics (e.g., kinetics) of practical catalysts and molecular understanding of the reaction.

Industrial utilizations of CO₂ as solvent and reactant amount to only 0.5 wt% (~128 Mt y⁻¹) of the total anthropogenic CO₂ emissions every year. In principle, chemical utilizations of CO₂ do not necessarily help mitigate the greenhouse effect considering energy input and carbon circulation. However, if CO₂ could be chemically transformed to fuels, it would be helpful to circulate carbon to alleviate the greenhouse effect. Particularly, production of fuels that can be easily stored and transported is preferable. Commercially, methanol is produced from synthesis gas, mainly containing CO and H₂ along with a small amount of CO₂ (~6 Mt y⁻¹) as the additive. Therefore, the utilization of CO₂-enriched

synthesis gas mixtures for CO₂ hydrogenation would be a potential process to chemical industries. From scientific standpoint, the development of catalysts with inexpensive metals such as iron and copper compounds which can also be active in mild conditions is a grand challenge. To reduce energy consumption, the introduction of electrochemical catalysis and solar energy with reactors not only breaks the reaction equilibrium but also supplies the hydrogen from water *in situ*. Moreover, permselective membrane can be used to isolate the by-product water, which deactivates catalysts and inhibits reaction rate, from the reaction systems. It is another challenge to look into the efficient hydrogenation of CO₃²⁻ or HCO₃³⁻ in a detailed manner considering availability and handling. Last but not least, the future research should certainly emphasize on the rational design of highly active catalyst and integral process to satisfy the economic development and sustainable utilization of carbon sources.

Acknowledgements

Financial support from the National Natural Science Foundation of China (21006068, 20936003, 21050110425), the Program for New Century Excellent Talents in University (NCET-04-0242), Seed Foundation of Tianjin University (60303002, 60307035), and the Program of Introducing Talents of Discipline to Universities (B06006) is gratefully acknowledged.

References

- 1 G. A. Olah, A. Goepfert and G. K. S. Prakash, *J. Org. Chem.*, 2009, **74**, 487–498.
- 2 X. D. Xu and J. A. Moulijn, *Energy Fuels*, 1996, **10**, 305–325.
- 3 S. N. Riduan and Y. G. Zhang, *Dalton Trans.*, 2010, **39**, 3347–3357.
- 4 J. Tollefson, *Nature*, 2009, **462**, 966–967.
- 5 H. Yang, Z. Xu, M. Fan, R. Gupta, R. B. Slimane, A. E. Bland and I. Wright, *J. Environ. Sci.*, 2008, **20**, 14–27.
- 6 M. Mikkelsen, M. Jorgensen and F. C. Krebs, *Energy Environ. Sci.*, 2010, **3**, 43–81.
- 7 A. J. Hunt, E. H. K. Sin, R. Marriott and J. H. Clark, *ChemSusChem*, 2010, **3**, 306–322.
- 8 G. Ferey, C. Serre, T. Devic, G. Maurin, H. Jobic, P. L. Llewellyn, G. De Weireld, A. Vimont, M. Daturi and J. S. Chang, *Chem. Soc. Rev.*, 2011, **40**, 550–562.
- 9 C. S. Song, *Catal. Today*, 2006, **115**, 2–32.
- 10 G. Centi and S. Perathoner, *Stud. Surf. Sci. Catal.*, 2004, **153**, 1–8.
- 11 J. Ma, N. N. Sun, X. L. Zhang, N. Zhao, F. K. Mao, W. Wei and Y. H. Sun, *Catal. Today*, 2009, **148**, 221–231.
- 12 A. Baiker, *Appl. Organomet. Chem.*, 2000, **14**, 751–762.
- 13 W. C. Chueh, C. Falter, M. Abbott, D. Scipio, P. Furler, S. M. Haile and A. Steinfeld, *Science*, 2010, **330**, 1797–1801.
- 14 I. Omae, *Catal. Today*, 2006, **115**, 33–52.
- 15 P. G. Jessop, F. Joo and C. C. Tai, *Coord. Chem. Rev.*, 2004, **248**, 2425–2442.
- 16 G. Centi and S. Perathoner, *Catal. Today*, 2009, **148**, 191–205.
- 17 W. L. Dai, S. L. Luo, S. F. Yin and C. T. Au, *Appl. Catal., A*, 2009, **366**, 2–12.
- 18 S. Zhang, Y. Chen, F. Li, X. Lu, W. Dai and R. Mori, *Catal. Today*, 2006, **115**, 61–69.
- 19 J. M. Sun, S. Fujita and M. Arai, *J. Organomet. Chem.*, 2005, **690**, 3490–3497.
- 20 P. G. Jessop, *J. Supercrit. Fluids*, 2006, **38**, 211–231.
- 21 H. Arakawa, M. Aresta, J. N. Armor, M. A. Barteau, E. J. Beckman, A. T. Bell, J. E. Bercaw, C. Creutz, E. Dinjus, D. A. Dixon, K. Domen, D. L. DuBois, J. Eckert, E. Fujita, D. H. Gibson, W. A. Goddard, D. W. Goodman, J. Keller,

- G. J. Kubas, H. H. Kung, J. E. Lyons, L. E. Manzer, T. J. Marks, K. Morokuma, K. M. Nicholas, R. Periana, L. Que, J. Rostrup-Nielsen, W. M. H. Sachtler, L. D. Schmidt, A. Sen, G. A. Somorjai, P. C. Stair, B. R. Stults and W. Tumas, *Chem. Rev.*, 2001, **101**, 953–996.
- 22 D. B. Dell'Amico, F. Calderazzo, L. Labella, F. Marchetti and G. Pampaloni, *Chem. Rev.*, 2003, **103**, 3857–3897.
- 23 M. Aresta and A. Dibenedetto, *Dalton Trans.*, 2007, 2975–2992.
- 24 T. Sakakura, J. C. Choi and H. Yasuda, *Chem. Rev.*, 2007, **107**, 2365–2387.
- 25 T. Sakakura and K. Kohno, *Chem. Commun.*, 2009, 1312–1330.
- 26 M. R. Kember, A. Buchard and C. K. Williams, *Chem. Commun.*, 2011, **47**, 141–163.
- 27 D. T. Whipple and P. J. A. Kenis, *J. Phys. Chem. Lett.*, 2010, **1**, 3451–3458.
- 28 E. E. Benson, C. P. Kubiak, A. J. Sathrum and J. M. Smieja, *Chem. Soc. Rev.*, 2009, **38**, 89–99.
- 29 P. G. Jessop, T. Ikariya and R. Noyori, *Chem. Rev.*, 1995, **95**, 259–272.
- 30 W. Leitner, *Angew. Chem., Int. Ed. Engl.*, 1995, **34**, 2207–2221.
- 31 C. Federsel, R. Jackstell and M. Beller, *Angew. Chem., Int. Ed.*, 2010, **49**, 6254–6257.
- 32 X. D. Xu and J. A. Moulijn, *Energy Fuels*, 1996, **10**, 305–325.
- 33 Y. Liu and D. Z. Liu, *Int. J. Hydrogen Energy*, 1999, **24**, 351–354.
- 34 F. S. Stone and D. Waller, *Top. Catal.*, 2003, **22**, 305–318.
- 35 C. S. Chen, W. H. Cheng and S. S. Lin, *Appl. Catal., A*, 2003, **238**, 55–67.
- 36 C. S. Chen, W. H. Cheng and S. S. Lin, *Chem. Commun.*, 2001, 1770–1771.
- 37 C. S. Chen, W. H. Cheng and S. S. Lin, *Appl. Catal., A*, 2004, **257**, 97–106.
- 38 C. S. Chen, J. H. Lin, J. H. You and C. R. Chen, *J. Am. Chem. Soc.*, 2006, **128**, 15950–15951.
- 39 A. Trovarelli, *Catal. Rev.*, 1996, **38**, 439–520.
- 40 L. H. Wang, S. X. Zhang and Y. A. Liu, *J. Rare Earths*, 2008, **26**, 66–70.
- 41 A. Goguet, F. Meunier, J. P. Breen, R. Burch, M. I. Petch and A. F. Ghenciu, *J. Catal.*, 2004, **226**, 382–392.
- 42 K. K. Bando, K. Soga, K. Kunimori and H. Arakawa, *Appl. Catal., A*, 1998, **175**, 67–81.
- 43 H. Kusama, K. K. Bando, K. Okabe and H. Arakawa, *Appl. Catal., A*, 2001, **205**, 285–294.
- 44 S. D. Kim and Y. Kang, *Chem. Eng. Sci.*, 1997, **52**, 3639–3660.
- 45 J. S. Kim, H. K. Kim, S. B. Lee, M. J. Choi, K. W. Lee and Y. Kang, *Korean J. Chem. Eng.*, 2001, **18**, 463–467.
- 46 G. Karagiannakis, S. Zisekas and M. Stoukides, *Solid State Ionics*, 2003, **162–163**, 313–318.
- 47 G. Pekridis, K. Kalimeri, N. Kaklidis, E. Vakouftsi, E. F. Iliopoulou, C. Athanasiou and G. E. Marnellos, *Catal. Today*, 2007, **127**, 337–346.
- 48 S. Bebelis, H. Karasali and C. G. Vayenas, *Solid State Ionics*, 2008, **179**, 1391–1395.
- 49 K. H. Ernst, C. T. Campbell and G. Moretti, *J. Catal.*, 1992, **134**, 66–74.
- 50 S. I. Fujita, M. Usui and N. Takezawa, *J. Catal.*, 1992, **134**, 220–225.
- 51 M. J. L. Ginés, A. J. Marchi and C. R. Apesteguía, *Appl. Catal., A*, 1997, **154**, 155–171.
- 52 C. S. Chen, W. H. Cheng and S. S. Lin, *Catal. Lett.*, 2000, **68**, 45–48.
- 53 C. S. Chen and W. H. Cheng, *Catal. Lett.*, 2002, **83**, 121–126.
- 54 C. S. Chen, J. H. Wu and T. W. Lai, *J. Phys. Chem. C*, 2010, **114**, 15021–15028.
- 55 F. Boccuzzi, A. Chiorino, G. Martra, M. Gargano, N. Ravasio and B. Carrozzini, *J. Catal.*, 1997, **165**, 129–139.
- 56 F. Coloma, F. Marquez, C. H. Rochester and J. A. Anderson, *Phys. Chem. Chem. Phys.*, 2000, **2**, 5320–5327.
- 57 V. Arunajatesan, B. Subramaniam, K. W. Hutchenson and F. E. Herkes, *Chem. Eng. Sci.*, 2007, **62**, 5062–5069.
- 58 D. Ferri, T. Burgi and A. Baiker, *Phys. Chem. Chem. Phys.*, 2002, **4**, 2667–2672.
- 59 A. Goguet, F. C. Meunier, D. Tibiletti, J. P. Breen and R. Burch, *J. Phys. Chem. B*, 2004, **108**, 20240–20246.
- 60 S. Qin, C. W. Hu, H. Q. Yang and Z. S. Su, *J. Phys. Chem. A*, 2005, **109**, 6498–6502.
- 61 C. Liu, L. Munjanja, T. R. Cundari and A. K. Wilson, *J. Phys. Chem. A*, 2010, **114**, 6207–6216.
- 62 P. J. Lunde and F. L. Kester, *Ind. Eng. Chem. Process Des. Dev.*, 1974, **13**, 27–33.
- 63 G. A. Du, S. Lim, Y. H. Yang, C. Wang, L. Pfeifferle and G. L. Haller, *J. Catal.*, 2007, **249**, 370–379.
- 64 J. N. Park and E. W. McFarland, *J. Catal.*, 2009, **266**, 92–97.
- 65 F. W. Chang, M. S. Kuo, M. T. Tsay and M. C. Hsieh, *Appl. Catal., A*, 2003, **247**, 309–320.
- 66 F. W. Chang, T. J. Hsiao, S. W. Chung and J. J. Lo, *Appl. Catal., A*, 1997, **164**, 225–236.
- 67 F. W. Chang, T. J. Hsiao and J. D. Shih, *Ind. Eng. Chem. Res.*, 1998, **37**, 3838–3845.
- 68 F. W. Chang, M. T. Tsay and S. P. Liang, *Appl. Catal., A*, 2001, **209**, 217–227.
- 69 G. D. Weatherbee and C. H. Bartholomew, *J. Catal.*, 1981, **68**, 67–76.
- 70 F. W. Chang, M. T. Tsay and M. S. Kuo, *Thermochim. Acta*, 2002, **386**, 161–172.
- 71 D. E. Peebles, D. W. Goodman and J. M. White, *J. Phys. Chem.*, 1983, **87**, 4378–4387.
- 72 C. K. Vance and C. H. Bartholomew, *Appl. Catal.*, 1983, **7**, 169–177.
- 73 M. Yamasaki, H. Habazaki, K. Asami, K. Izumiya and K. Hashimoto, *Catal. Commun.*, 2006, **7**, 24–28.
- 74 F. Ocampo, B. Louis and A. C. Roger, *Appl. Catal., A*, 2009, **369**, 90–96.
- 75 N. Perkas, G. Amirian, Z. Y. Zhong, J. Teo, Y. Gofer and A. Gedanken, *Catal. Lett.*, 2009, **130**, 455–462.
- 76 S. Sane, J. M. Bonnier, J. P. Damon and J. Masson, *Appl. Catal.*, 1984, **9**, 69–83.
- 77 G. D. Lee, M. J. Moon, J. H. Park, S. S. Park and S. S. Hong, *Korean J. Chem. Eng.*, 2005, **22**, 541–546.
- 78 J. Sehested, K. E. Larsen, A. L. Kustov, A. M. Frey, T. Johannessen, T. Bligaard, M. P. Andersson, J. K. Norskov and C. H. Christensen, *Top. Catal.*, 2007, **45**, 9–13.
- 79 M. Agnelli, M. Kolb and C. Mirodatos, *J. Catal.*, 1994, **148**, 9–21.
- 80 A. L. Kustov, A. M. Frey, K. E. Larsen, T. Johannessen, J. K. Norskov and C. H. Christensen, *Appl. Catal., A*, 2007, **320**, 98–104.
- 81 Z. Kowalczyk, K. Stolecki, W. Rarog-Pilecka, E. Miskiewicz, E. Wilczkowska and Z. Karpinski, *Appl. Catal., A*, 2008, **342**, 35–39.
- 82 T. Abe, M. Tanizawa, K. Watanabe and A. Taguchi, *Energy Environ. Sci.*, 2009, **2**, 315–321.
- 83 L. T. Luo, S. J. Li and Y. Zhu, *J. Serb. Chem. Soc.*, 2005, **70**, 1419–1425.
- 84 M. Kusmierz, *Catal. Today*, 2008, **137**, 429–432.
- 85 K. P. Yu, W. Y. Yu, M. C. Ku, Y. C. Liou and S. H. Chien, *Appl. Catal., B*, 2008, **84**, 112–118.
- 86 T. Szailer, E. Novak, A. Oszko and A. Erdohelyi, *Top. Catal.*, 2007, **46**, 79–86.
- 87 C. G. Vayenas and C. G. Koutsodontis, *J. Chem. Phys.*, 2008, **128**, 182506–182518.
- 88 S. Bebelis, H. Karasali and C. G. Vayenas, *J. Appl. Electrochem.*, 2008, **38**, 1127–1133.
- 89 E. I. Papaioannou, S. Souentie, A. Hammad and C. G. Vayenas, *Catal. Today*, 2009, **146**, 336–344.
- 90 J. L. Falconer and A. E. Zagli, *J. Catal.*, 1980, **62**, 280–285.
- 91 G. D. Weatherbee and C. H. Bartholomew, *J. Catal.*, 1982, **77**, 460–472.
- 92 D. E. Peebles, D. W. Goodman and J. M. White, *J. Phys. Chem.*, 1983, **87**, 4378–4387.
- 93 M. Marwood, R. Doepper and A. Renken, *Appl. Catal., A*, 1997, **151**, 223–246.
- 94 A. L. Lapidus, N. A. Gaidai, N. V. Nekrasov, L. A. Tishkova, Y. A. Agafonov and T. N. Myshenkova, *Pet. Chem.*, 2007, **47**, 75–82.
- 95 S. Fujita, H. Terunuma, H. Kobayashi and N. Takezawa, *React. Kinet. Catal. Lett.*, 1987, **33**, 179–184.
- 96 C. Schild, A. Wokaun and A. Baiker, *J. Mol. Catal.*, 1990, **63**, 243–254.
- 97 J. Sehested, S. Dahl, J. Jacobsen and J. R. Rostrup-Nielsen, *J. Phys. Chem. B*, 2005, **109**, 2432–2438.

- 98 R. M. Watwe, H. S. Bengaard, J. R. Rostrup-Nielsen, J. A. Dumesic and J. K. Nørskov, *J. Catal.*, 2000, **189**, 16–30.
- 99 M. Ackermann, O. Robach, C. Walker, C. Quiros, H. Isern and S. Ferrer, *Surf. Sci.*, 2004, **557**, 21–30.
- 100 S. J. Choe, H. J. Kang, S. J. Kim, S. B. Park, D. H. Park and D. S. Huh, *Bull. Korean Chem. Soc.*, 2005, **26**, 1682–1688.
- 101 H. Y. Kim, H. M. Lee and J. N. Park, *J. Phys. Chem. C*, 2010, **114**, 7128–7131.
- 102 N. Blangenois, M. Jacquemin and P. Ruiz, *WO 2010006386*, 2010, 56.
- 103 M. Jacquemin, A. Beuls and P. Ruiz, *Catal. Today*, 2010, **157**, 462–466.
- 104 K. Fujimoto and T. Shikada, *Appl. Catal.*, 1987, **31**, 13–23.
- 105 J. F. Lee, W. S. Chern, M. D. Lee and T. Y. Dong, *Can. J. Chem. Eng.*, 2009, **70**, 511–515.
- 106 P. S. S. Prasad, J. W. Bae, K. W. Jun and K. W. Lee, *Catal. Surv. Asia*, 2008, **12**, 170–183.
- 107 M. Fujiwara, R. Kieffer, H. Ando and Y. Souma, *Appl. Catal., A*, 1995, **121**, 113–124.
- 108 R. W. Dorner, D. R. Hardy, F. W. Williams, B. H. Davis and H. D. Willauer, *Energy Fuels*, 2009, **23**, 4190–4195.
- 109 Y. Q. Zhang, G. Jacobs, D. E. Sparks, M. E. Dry and B. H. Davis, *Catal. Today*, 2002, **71**, 411–418.
- 110 A. N. Akin, M. Ataman, A. E. Aksoylu and Z. I. Önsan, *React. Kinet. Catal. Lett.*, 2002, **76**, 265–270.
- 111 T. Riedel, M. Claeys, H. Schulz, G. Schaub, S. S. Nam, K. W. Jun, M. J. Choi, G. Kishan and K. W. Lee, *Appl. Catal., A*, 1999, **186**, 201–213.
- 112 F. Tihay, A. C. Roger, G. Pourroy and A. Kiennemann, *Energy Fuels*, 2002, **16**, 1271–1276.
- 113 C. G. Visconti, L. Lietti, E. Tronconi, P. Forzatti, R. Zennaro and E. Finocchio, *Appl. Catal., A*, 2009, **355**, 61–68.
- 114 D. S. Newsome, *Catal. Rev.*, 1980, **21**, 275–318.
- 115 H. Schulz, *Appl. Catal., A*, 1999, **186**, 3–12.
- 116 G. P. Van Der Laan and A. A. C. M. Beenackers, *Catal. Rev. Sci. Eng.*, 1999, **41**, 255–318.
- 117 M. E. Dry, *Appl. Catal., A*, 1996, **138**, 319–344.
- 118 L. Xu, S. Bao, R. J. O'Brien, A. Rajee and B. H. Davis, *Chem. Technol.*, 1998, **28**, 47–53.
- 119 Y. Jin and A. K. Datye, *J. Catal.*, 2000, **196**, 8–17.
- 120 S. R. Yan, K. W. Jun, J. S. Hong, S. B. Lee, M. J. Choi and K. W. Lee, *Korean J. Chem. Eng.*, 1999, **16**, 357–361.
- 121 M. L. Cubeiro, H. Morales, M. R. Goldwasser, M. J. Pérez-Zurita and F. González-Jiménez, *React. Kinet. Catal. Lett.*, 2000, **69**, 259–264.
- 122 T. Riedel, G. Schaub, K. W. Jun and K. W. Lee, *Ind. Eng. Chem. Res.*, 2001, **40**, 1355–1363.
- 123 K. W. Jun, H. S. Roh, K. S. Kim, J. S. Ryu and K. W. Lee, *Appl. Catal., A*, 2004, **259**, 221–226.
- 124 H. Schulz, T. Riedel and G. Schaub, *Top. Catal.*, 2005, **32**, 117–124.
- 125 T. Riedel, H. Schulz, G. Schaub, K. W. Jun, J. S. Hwang and K. W. Lee, *Top. Catal.*, 2003, **26**, 41–54.
- 126 S. C. Lee, J. S. Kim, W. C. Shin, M. J. Choi and S. J. Choung, *J. Mol. Catal. A: Chem.*, 2009, **301**, 98–105.
- 127 M. Niemela and M. Nokkosmaki, *Catal. Today*, 2005, **100**, 269–274.
- 128 T. Herranz, S. Rojas, F. J. Perez-Alonso, A. Ojeda, P. Terreros and J. L. G. Fierro, *Appl. Catal., A*, 2006, **311**, 66–75.
- 129 W. S. Ning, N. Koizumi and M. Yamada, *Energy Fuels*, 2009, **23**, 4696–4700.
- 130 R. W. Dorner, D. R. Hardy, F. W. Williams and H. D. Willauer, *Appl. Catal. A: Gen.*, 2010, **373**, 112–121.
- 131 W. P. Ma, Y. L. Zhao, Y. W. Li, Y. Y. Xu and J. L. Zhou, *React. Kinet. Catal. Lett.*, 1999, **66**, 217–223.
- 132 L. Y. Xu, Q. X. Wang, D. B. Liang, X. Wang, L. W. Lin, W. Cui and Y. D. Xu, *Appl. Catal., A*, 1998, **173**, 19–25.
- 133 J. Abbott, N. J. Clark and B. G. Baker, *Appl. Catal.*, 1986, **26**, 141–153.
- 134 T. Li, Y. Yang, C. Zhang, X. An, H. Wan, Z. Tao, H. Xiang, Y. Li, F. Yi and B. Xu, *Fuel*, 2007, **86**, 921–928.
- 135 H. Ando, Q. Xu, M. Fujiwara, Y. Matsumura, M. Tanaka and Y. Souma, *Catal. Today*, 1998, **45**, 229–234.
- 136 Q. Fu, H. Saltsburg and M. Flytzani-Stephanopoulos, *Science*, 2003, **301**, 935–938.
- 137 F. J. Perez-Alonso, M. Ojeda, T. Herranz, S. Rojas, J. M. Gonzalez-Carballo, P. Terreros and J. L. G. Fierro, *Catal. Commun.*, 2008, **9**, 1945–1948.
- 138 R. W. Dorner, D. R. Hardy, F. W. Williams and H. D. Willauer, *Catal. Commun.*, 2010, **11**, 816–819.
- 139 X. M. Ni, Y. S. Tan, Y. Z. Han and N. Tsubaki, *Catal. Commun.*, 2007, **8**, 1711–1714.
- 140 B. Rongxian, T. Yisheng and H. Yizhuo, *Fuel Process. Technol.*, 2004, **86**, 293–301.
- 141 S. C. Lee, J. H. Jang, B. Y. Lee, J. S. Kim, M. Kang, S. B. Lee, M. J. Choi and S. J. Choung, *J. Mol. Catal. A: Chem.*, 2004, **210**, 131–141.
- 142 S. S. Nam, G. Kishan, M. W. Lee, M. J. Choi and K. W. Lee, *Appl. Organomet. Chem.*, 2000, **14**, 794–798.
- 143 S. R. Yan, K. W. Jun, J. S. Hong, M. J. Choi and K. W. Lee, *Appl. Catal., A*, 2000, **194–195**, 63–70.
- 144 G. Zhao, C. Zhang, S. Qin, H. Xiang and Y. Li, *J. Mol. Catal. A: Chem.*, 2008, **286**, 137–142.
- 145 S. C. Lee, J. H. Jang, B. Y. Lee, M. C. Kang, M. Kang and S. J. Choung, *Appl. Catal., A*, 2003, **253**, 293–304.
- 146 M. P. Rohde, D. Unruh and G. Schaub, *Ind. Eng. Chem. Res.*, 2005, **44**, 9653–9658.
- 147 M. P. Rohde, D. Unruh and G. Schaub, *Catal. Today*, 2005, **106**, 143–148.
- 148 J. S. Kim, S. Lee, S. B. Lee, M. J. Choi and K. W. Lee, *Catal. Today*, 2006, **115**, 228–234.
- 149 T. Inui and T. Takeguchi, *Catal. Today*, 1991, **10**, 95–106.
- 150 B. J. Liaw and Y. Z. Chen, *Appl. Catal., A*, 2001, **206**, 245–256.
- 151 F. Arena, K. Barbera, G. Italiano, G. Bonura, L. Spadaro and F. Frusteri, *J. Catal.*, 2007, **249**, 185–194.
- 152 M. Saito and K. Murata, *Catal. Surv. Asia*, 2004, **8**, 285–294.
- 153 X. M. Liu, G. Q. Lu, Z. F. Yan and J. Beltramini, *Ind. Eng. Chem. Res.*, 2003, **42**, 6518–6530.
- 154 J. Toyir, P. R. de la Piscina, J. L. G. Fierro and N. Homs, *Appl. Catal., B*, 2001, **29**, 207–215.
- 155 J. Toyir, P. Ramirez de la Piscina, J. L. G. Fierro and N. Homs, *Appl. Catal., B*, 2001, **34**, 255–266.
- 156 J. Liu, J. Shi, D. He, Q. Zhang, X. Wu, Y. Liang and Q. Zhu, *Appl. Catal., A*, 2001, **218**, 113–119.
- 157 X. M. Liu, G. Q. Lu and Z. F. Yan, *Appl. Catal., A*, 2005, **279**, 241–245.
- 158 J. Sloczynski, R. Grabowski, P. Olszewski, A. Kozłowska, J. Stoch, M. Lachowska and J. Skrzypek, *Appl. Catal., A*, 2006, **310**, 127–137.
- 159 R. Raudaskoski, M. V. Niemela and R. L. Keiski, *Top. Catal.*, 2007, **45**, 57–60.
- 160 X. M. Guo, D. S. Mao, S. Wang, G. S. Wu and G. Z. Lu, *Catal. Commun.*, 2009, **10**, 1661–1664.
- 161 J. Sloczynski, R. Grabowski, A. Kozłowska, P. Olszewski, J. Stoch, J. Skrzypek and M. Lachowska, *Appl. Catal., A*, 2004, **278**, 11–23.
- 162 X. M. Guo, D. S. Mao, G. Z. Lu, S. Wang and G. S. Wu, *J. Catal.*, 2010, **271**, 178–185.
- 163 X. An, J. L. Li, Y. Z. Zuo, Q. Zhang, D. Z. Wang and J. F. Wang, *Catal. Lett.*, 2007, **118**, 264–269.
- 164 X. L. Liang, X. Dong, G. D. Lin and H. B. Zhang, *Appl. Catal., B*, 2009, **88**, 315–322.
- 165 S. E. Collins, D. L. Chiavassa, A. L. Bonivardi and M. A. Baltanas, *Catal. Lett.*, 2005, **103**, 83–88.
- 166 L. S. Jia, J. Gao, W. P. Fang and Q. B. Li, *Catal. Commun.*, 2009, **10**, 2000–2003.
- 167 J. Yoshihara and C. T. Campbell, *J. Catal.*, 1996, **161**, 776–782.
- 168 C. V. Ovesen, B. S. Clausen, J. Schiøtz, P. Stoltze, H. Topsøe and J. K. Nørskov, *J. Catal.*, 1997, **168**, 133–142.
- 169 S. Fujita, S. Moribe, Y. Kanamori, M. Kakudate and N. Takezawa, *Appl. Catal., A*, 2001, **207**, 121–128.
- 170 J. Nakamura, Y. Choi and T. Fujitani, *Top. Catal.*, 2003, **22**, 277–285.
- 171 A. A. Ponce and K. J. Klabunde, *J. Mol. Catal. A: Chem.*, 2005, **225**, 1–6.
- 172 I. Melian-Cabrera, M. L. Granados and J. L. G. Fierro, *J. Catal.*, 2002, **210**, 273–284.
- 173 I. Melian-Cabrera, M. L. Granados and J. L. G. Fierro, *J. Catal.*, 2002, **210**, 285–294.
- 174 F. Arena, G. Italiano, K. Barbera, S. Bordiga, G. Bonura, L. Spadaro and F. Frusteri, *Appl. Catal., A*, 2008, **350**, 16–23.

- 175 F. Arena, G. Italiano, K. Barbera, G. Bonura, L. Spadaro and F. Frusteri, *Catal. Today*, 2009, **143**, 80–85.
- 176 K. T. Jung and A. T. Bell, *Catal. Lett.*, 2002, **80**, 63–68.
- 177 J. Sloczynski, R. Grabowski, A. Kozłowska, P. Olszewski, M. Lachowska, J. Skrzypek and J. Stoch, *Appl. Catal., A*, 2003, **249**, 129–138.
- 178 I. A. Fisher and A. T. Bell, *J. Catal.*, 1997, **172**, 222–237.
- 179 K.-D. Jung and A. T. Bell, *J. Catal.*, 2000, **193**, 207–223.
- 180 S. E. Collins, M. A. Baltanás, J. L. Garcia Fierro and A. L. Bonivardi, *J. Catal.*, 2002, **211**, 252–264.
- 181 D. L. Chiavassa, J. Barrandeguy, A. L. Bonivardi and M. A. Baltanas, *Catal. Today*, 2008, **133–135**, 780–786.
- 182 D. K. Lee, D. S. Kim and S. W. Kim, *Appl. Organomet. Chem.*, 2001, **15**, 148–150.
- 183 D. W. Stephan, *Dalton Trans.*, 2009, 3129–3136.
- 184 C. M. Mömning, S. Frömel, G. Kehr, R. Fröhlich, S. Grimme and G. Erker, *J. Am. Chem. Soc.*, 2009, **131**, 12280–12289.
- 185 M. Ullrich, K. S. H. Seto, A. J. Lough and D. W. Stephan, *Chem. Commun.*, 2009, 2335–2337.
- 186 P. Spies, S. Schwendemann, S. Lange, G. Kehr, R. Fröhlich and G. Erker, *Angew. Chem.*, 2008, **120**, 7654–7657.
- 187 A. E. Ashley, A. L. Thompson and D. O'Hare, *Angew. Chem., Int. Ed.*, 2009, **48**, 9839–9843.
- 188 M. R. Rahimpour, *Fuel Process. Technol.*, 2008, **89**, 556–566.
- 189 M. R. Rahimpour and K. Alizadehhesari, *Int. J. Hydrogen Energy*, 2009, **34**, 1349–1362.
- 190 M. R. Rahimpour and S. Ghader, *Chem. Eng. Process.*, 2004, **43**, 1181–1188.
- 191 R. P. W. J. Struis and S. Stucki, *Appl. Catal., A*, 2001, **216**, 117–129.
- 192 G. Chen and Q. Yuan, *Sep. Purif. Technol.*, 2004, **34**, 227–237.
- 193 G. Barbieri, G. Marigliano, G. Golemme and E. Drioli, *Chem. Eng. J.*, 2002, **85**, 53–59.
- 194 F. Gallucci, L. Paturzo and A. Basile, *Chem. Eng. Process.*, 2004, **43**, 1029–1036.
- 195 F. Gallucci and A. Basile, *Int. J. Hydrogen Energy*, 2007, **32**, 5050–5058.
- 196 V. M. Palekar, H. Jung, J. W. Tiemey and I. Wender, *Appl. Catal., A*, 1993, **102**, 13–34.
- 197 A. Cybulski, *Catal. Rev.*, 1994, **36**, 557–615.
- 198 P. J. A. Tijn, F. J. Waller and D. M. Brown, *Appl. Catal., A*, 2001, **221**, 275–282.
- 199 S. G. Lee and A. Sardesai, *Top. Catal.*, 2005, **32**, 197–207.
- 200 X. B. Zhang, L. Zhong, Q. H. Guo, H. Fan, H. Y. Zheng and K. C. Xie, *Fuel*, 2010, **89**, 1348–1352.
- 201 Y. Liu, Y. Zhang, T. J. Wang and N. Tsubaki, *Chem. Lett.*, 2007, **36**, 1182–1183.
- 202 Y. Borodko and G. A. Somorjai, *Appl. Catal., A*, 1999, **186**, 355–362.
- 203 R. A. Koeppel, A. Baiker and A. Wokaun, *Appl. Catal., A*, 1992, **84**, 77–102.
- 204 W. P. A. Jansen, J. Beckers, J. C. Van der Heuvel, A. W. D. Van der Gon, A. Bliet and H. H. Brongersma, *J. Catal.*, 2002, **210**, 229–236.
- 205 M. Saito, T. Fujitani, M. Takeuchi and T. Watanabe, *Appl. Catal., A*, 1996, **138**, 311–318.
- 206 S. H. Liu, H. P. Wang, H. C. Wang and Y. W. Yang, *J. Electron Spectrosc. Relat. Phenom.*, 2005, **144–147**, 373–376.
- 207 Q. L. Tang, Q. J. Hong and Z. P. Liu, *J. Catal.*, 2009, **263**, 114–122.
- 208 T. C. Schilke, I. A. Fisher and A. T. Bell, *J. Catal.*, 1999, **184**, 144–156.
- 209 K. D. Jung and A. T. Bell, *J. Catal.*, 2000, **193**, 207–223.
- 210 D. L. Chiavassa, S. E. Collins, A. L. Bonivardi and M. A. Baltanas, *Chem. Eng. J.*, 2009, **150**, 204–212.
- 211 H. W. Lim, M. J. Park, S. H. Kang, H. J. Chae, J. W. Bae and K. W. Jun, *Ind. Eng. Chem. Res.*, 2009, **48**, 10448–10455.
- 212 M. Bowker, R. A. Hadden, H. Houghton, J. N. K. Hyland and K. C. Waugh, *J. Catal.*, 1988, **109**, 263–273.
- 213 J. Tabatabaei, B. H. Sakakini and K. C. Waugh, *Catal. Lett.*, 2006, **110**, 77–84.
- 214 J. Weigel, R. A. Koeppel, A. Baiker and A. Wokaun, *Langmuir*, 1996, **12**, 5319–5329.
- 215 Y. Nitta, O. Suwata, Y. Ikeda, Y. Okamoto and T. Imanaka, *Catal. Lett.*, 1994, **26**, 345–354.
- 216 S. E. Collins, M. A. Baltanas and A. L. Bonivardi, *J. Catal.*, 2004, **226**, 410–421.
- 217 Y. X. Yang, J. Evans, J. A. Rodriguez, M. G. White and P. Liu, *Phys. Chem. Chem. Phys.*, 2010, **12**, 9909–9917.
- 218 P. Liu, Y. Choi, Y. X. Yang and M. G. White, *J. Phys. Chem. A*, 2010, **114**, 3888–3895.
- 219 B. Chan and L. Radom, *J. Am. Chem. Soc.*, 2006, **128**, 5322–5323.
- 220 B. Chan and L. Radom, *J. Am. Chem. Soc.*, 2008, **130**, 9790–9799.
- 221 R. A. Koppel, C. Stocker and A. Baiker, *J. Catal.*, 1998, **179**, 515–527.
- 222 F. Yariipour, F. Baghaei, I. Schmidt and J. Perregaard, *Catal. Commun.*, 2005, **6**, 542–549.
- 223 A. T. Aguayo, J. Erena, D. Mier, J. M. Arandes, M. Olazar and J. Bilbao, *Ind. Eng. Chem. Res.*, 2007, **46**, 5522–5530.
- 224 T. Wang, J. Wang and Y. Jin, *Ind. Eng. Chem. Res.*, 2007, **46**, 5824–5847.
- 225 T. A. Semelsberger, K. C. Ott, R. L. Borup and H. L. Greene, *Appl. Catal., A*, 2006, **309**, 210–223.
- 226 M. Nilsson, L. J. Pettersson and B. Lindström, *Energy Fuels*, 2006, **20**, 2164–2169.
- 227 J. L. Tao, K. W. Jun and K. W. Lee, *Appl. Organomet. Chem.*, 2001, **15**, 105–108.
- 228 S. Wang, D. S. Mao, X. M. Guo, G. S. Wu and G. Z. Lu, *Catal. Commun.*, 2009, **10**, 1367–1370.
- 229 X. An, Y. Z. Zuo, Q. Zhang, D. Z. Wang and J. F. Wang, *Ind. Eng. Chem. Res.*, 2008, **47**, 6547–6554.
- 230 J. Erena, R. Garona, J. M. Arandes, A. T. Aguayo and J. Bilbao, *Catal. Today*, 2005, **107–108**, 467–473.
- 231 G. X. Qi, J. H. Fei, X. M. Zheng and Z. Y. Hou, *Catal. Lett.*, 2001, **72**, 121–124.
- 232 K. P. Sun, W. W. Lu, M. Wang and X. L. Xu, *Catal. Commun.*, 2004, **5**, 367–370.
- 233 K. W. Jun, K. S. R. Rao, M. H. Jung and K. W. Lee, *Bull. Korean Chem. Soc.*, 1998, **19**, 466–470.
- 234 A. T. Aguayo, J. Erena, I. Sierra, M. Olazar and J. Bilbao, *Catal. Today*, 2005, **106**, 265–270.
- 235 T. Takeguchi, K. Yanagisawa, T. Inui and M. Inoue, *Appl. Catal., A*, 2000, **192**, 201–209.
- 236 Q. Zhang, Y. Z. Zuo, M. H. Han, J. F. Wang, Y. Jin and F. Wei, *Catal. Today*, 2010, **150**, 55–60.
- 237 M. Stöcker, *Microporous Mesoporous Mater.*, 1999, **29**, 3–48.
- 238 V. Vishwanathan, K. W. Jun, J. W. Kim and H. S. Roh, *Appl. Catal., A*, 2004, **276**, 251–255.
- 239 X. D. Peng, B. A. Toseland and P. J. A. Tijn, *Chem. Eng. Sci.*, 1999, **54**, 2787–2792.
- 240 K. L. Ng, D. Chadwick and B. A. Toseland, *Chem. Eng. Sci.*, 1999, **54**, 3587–3592.
- 241 W. J. Shen, K. W. Jun, H. S. Choi and K. W. Lee, *Korean J. Chem. Eng.*, 2000, **17**, 210–216.
- 242 G. X. Jia, Y. S. Tan and Y. Z. Han, *Ind. Eng. Chem. Res.*, 2006, **45**, 1152–1159.
- 243 H. Kurakata, Y. Izumi and K. Aika, *Chem. Commun.*, 1996, 389–390.
- 244 H. Kusama, K. Okabe, K. Sayama and H. Arakawa, *Catal. Today*, 1996, **28**, 261–266.
- 245 Y. Izumi, *Platinum Met. Rev.*, 1997, **41**, 166.
- 246 H. Kusama, K. Okabe, K. Sayama and H. Arakawa, *Energy*, 1997, **22**, 343–348.
- 247 T. Inui and T. Yamamoto, *Catal. Today*, 1998, **45**, 209–214.
- 248 Y. Izumi, H. Kurakata and K. Aika, *J. Catal.*, 1998, **175**, 236–244.
- 249 T. Inui, T. Yamamoto, M. Inoue, H. Hara, T. Takeguchi and J. B. Kim, *Appl. Catal., A*, 1999, **186**, 395–406.
- 250 K. Higuchi, Y. Haneda, K. Tabata, Y. Nakahara and M. Takagawa, *Stud. Surf. Sci. Catal.*, 1998, **114**, 517–520.
- 251 M. Takagawa, A. Okamoto, H. Fujimura, Y. Izawa and H. Arakawa, *Stud. Surf. Sci. Catal.*, 1998, **114**, 525–528.
- 252 Y. Izumi, K. Asakura and Y. Iwasawa, *J. Catal.*, 1991, **127**, 631–644.
- 253 Y. Izumi and Y. Iwasawa, *J. Phys. Chem.*, 1992, **96**, 10942–10948.
- 254 K.-i. Tominaga and Y. Sasaki, *Catal. Commun.*, 2000, **1**, 1–3.
- 255 K.-i. Tominaga and Y. Sasaki, *J. Mol. Catal. A: Chem.*, 2004, **220**, 159–165.
- 256 Y. Hashimoto and A. Ayame, *Appl. Catal., A*, 2003, **250**, 247–254.

- 257 S. I. Fujita, S. Okamura, Y. Akiyama and M. Arai, *Int. J. Mol. Sci.*, 2007, **8**, 749–759.
- 258 K. Tominaga, *Catal. Today*, 2006, **115**, 70–72.
- 259 M. L. Kontkanen, L. Oresmaa, M. A. Moreno, J. Janis, E. Laurila and M. Haukka, *Appl. Catal., A*, 2009, **365**, 130–134.
- 260 Z. F. Zhang, S. Q. Hu, J. L. Song, W. J. Li, G. Y. Yang and B. X. Han, *ChemSusChem*, 2009, **2**, 234–238.
- 261 T. C. Johnson, D. J. Morris and M. Wills, *Chem. Soc. Rev.*, 2010, **39**, 81–88.
- 262 N. N. Ezhova, N. V. Kolesnichenko, A. V. Bulygin, E. V. Slivinskii and S. Han, *Russ. Chem. Bull.*, 2002, **51**, 2165–2169.
- 263 Y. Gao, J. K. Kuncheria, H. A. Jenkins, R. J. Puddephatt and G. P. A. Yap, *J. Chem. Soc., Dalton Trans.*, 2000, 3212–3217.
- 264 M. L. Man, Z. Y. Zhou, S. M. Ng and C. P. Lau, *Dalton Trans.*, 2003, 3727–3735.
- 265 C. Q. Yin, Z. T. Xu, S. Y. Yang, S. M. Ng, K. Y. Wong, Z. Y. Lin and C. P. Lau, *Organometallics*, 2001, **20**, 1216–1222.
- 266 S. M. Ng, C. Q. Yin, C. H. Yeung, T. C. Chan and C. P. Lau, *Eur. J. Inorg. Chem.*, 2004, 1788–1793.
- 267 P. G. Jessop, Y. Hsiao, T. Ikariya and R. Noyori, *J. Am. Chem. Soc.*, 1996, **118**, 344–355.
- 268 P. Munshi, A. D. Main, J. C. Linehan, C. C. Tai and P. G. Jessop, *J. Am. Chem. Soc.*, 2002, **124**, 7963–7971.
- 269 T. T. Thai, B. Therrien and G. Suss-Fink, *J. Organomet. Chem.*, 2009, **694**, 3973–3981.
- 270 S. Sanz, A. Azua and E. Peris, *Dalton Trans.*, 2010, **39**, 6339–6343.
- 271 Y. Himeda, *Eur. J. Inorg. Chem.*, 2007, 3927–3941.
- 272 R. Tanaka, M. Yamashita and K. Nozaki, *J. Am. Chem. Soc.*, 2009, **131**, 14168–14169.
- 273 S. Sanz, M. Benitez and E. Peris, *Organometallics*, 2010, **29**, 275–277.
- 274 C. C. Tai, T. Chang, B. Roller and P. G. Jessop, *Inorg. Chem.*, 2003, **42**, 7340–7341.
- 275 Y. Zhang, J. Fei, Y. Yu and X. Zheng, *Catal. Commun.*, 2004, **5**, 643–646.
- 276 Y. Inoue, H. Izumida, Y. Sasaki and H. Hashimoto, *Chem. Lett.*, 1976, 863–864.
- 277 C. C. Tai, J. Pitts, J. C. Linehan, A. D. Main, P. Munshi and P. G. Jessop, *Inorg. Chem.*, 2002, **41**, 1606–1614.
- 278 J. C. Tsai and K. M. Nicholas, *J. Am. Chem. Soc.*, 1992, **114**, 5117–5124.
- 279 M. Iwatani, K. Kudo, N. Sugita and Y. Takezaki, *J. Jpn. Pet. Inst.*, 1978, **21**, 290–296.
- 280 E. R. Pérez, M. O. da Silva, V. C. Costa, U. P. Rodrigues-Filho and D. W. Franco, *Tetrahedron Lett.*, 2002, **43**, 4091–4093.
- 281 P. G. Jessop, T. Ikariya and R. Noyori, *Nature*, 1994, **368**, 231–233.
- 282 C. A. Thomas, R. J. Bonilla, Y. Huang and P. G. Jessop, *Can. J. Chem.*, 2001, **79**, 719–724.
- 283 Y. Himeda, N. Onozawa-Komatsuzaki, H. Sugihara and K. Kasuga, *Organometallics*, 2007, **26**, 702–712.
- 284 Y. Himeda, N. Onozawa-Komatsuzaki, H. Sugihara and K. Kasuga, *J. Am. Chem. Soc.*, 2005, **127**, 13118–13119.
- 285 H. Hayashi, S. Ogo and S. Fukuzumi, *Chem. Commun.*, 2004, 2714–2715.
- 286 K. Merz, M. Moreno, E. Löffler, L. Khodeir, A. Rittermeier, K. Fink, K. Kotsis, M. Muhler and M. Driess, *Chem. Commun.*, 2008, 73–75.
- 287 O. Krocher, R. A. Koppel and A. Baiker, *Chem. Commun.*, 1997, 453–454.
- 288 R. Fornika, H. Gorls, B. Seemann and W. Leitner, *J. Chem. Soc., Chem. Commun.*, 1995, 1479–1481.
- 289 K. M. K. Yu, C. M. Y. Yeung and S. C. Tsang, *J. Am. Chem. Soc.*, 2007, **129**, 6360–6361.
- 290 S. C. Tsang, C. D. A. Bulpitt, P. C. H. Mitchell and A. J. Ramirez-Cuesta, *J. Phys. Chem. B*, 2001, **105**, 5737–5742.
- 291 Z. F. Zhang, E. Xie, W. J. Li, S. Q. Hu, J. L. Song, T. Jiang and B. X. Han, *Angew. Chem., Int. Ed.*, 2008, **47**, 1127–1129.
- 292 M. K. Whittlesey, R. N. Perutz and M. H. Moore, *Organometallics*, 1996, **15**, 5166–5169.
- 293 Y. Musashi and S. Sakaki, *J. Am. Chem. Soc.*, 2000, **122**, 3867–3877.
- 294 Y. Y. Ohnishi, T. Matsunaga, Y. Nakao, H. Sato and S. Sakaki, *J. Am. Chem. Soc.*, 2005, **127**, 4021–4032.
- 295 A. Urakawa, F. Jutz, G. Laurency and A. Baiker, *Chem.–Eur. J.*, 2007, **13**, 3886–3899.
- 296 Y. Musashi and S. Sakaki, *J. Am. Chem. Soc.*, 2002, **124**, 7588–7603.
- 297 W. Leitner, E. Dinjus and F. Gaßner, *J. Organomet. Chem.*, 1994, **475**, 257–266.
- 298 F. Hutschka, A. Dedieu, M. Eichberger, R. Fornika and W. Leitner, *J. Am. Chem. Soc.*, 1997, **119**, 4432–4443.
- 299 A. Urakawa, M. Iannuzzi, J. Hutter and A. Baiker, *Chem.–Eur. J.*, 2007, **13**, 6828–6840.
- 300 A. D. Getty, C. C. Tai, J. C. Linehan, P. G. Jessop, M. M. Olmstead and A. L. Rheingold, *Organometallics*, 2009, **28**, 5466–5477.
- 301 M. S. G. Ahlquist, *J. Mol. Catal. A: Chem.*, 2010, **324**, 3–8.
- 302 Y. Y. Ohnishi, Y. Nakao, H. Sato and S. Sakaki, *Organometallics*, 2006, **25**, 3352–3363.
- 303 S. Ogo, R. Kabe, H. Hayashi, R. Harada and S. Fukuzumi, *Dalton Trans.*, 2006, 4657–4663.
- 304 P. G. Jessop, Y. Hsiao, T. Ikariya and R. Noyori, *J. Am. Chem. Soc.*, 1994, **116**, 8851–8852.
- 305 O. Krocher, R. A. Koppel and A. Baiker, *Chem. Commun.*, 1996, 1497–1498.
- 306 L. Schmid, M. Rohr and A. Baiker, *Chem. Commun.*, 1999, 2303–2304.
- 307 F. Liu, M. B. Abrams, R. T. Baker and W. Tumas, *Chem. Commun.*, 2001, 433–434.
- 308 J. L. Liu, C. K. Guo, Z. F. Zhang, T. Jiang, H. Z. Liu, J. L. Song, H. L. Fan and B. X. Han, *Chem. Commun.*, 2010, **46**, 5770–5772.
- 309 Y. Kayaki, T. Suzuki and T. Ikariya, *Chem. Lett.*, 2001, 1016–1017.
- 310 Y. Kayaki, Y. Shimokawatoko and T. Ikariya, *Inorg. Chem.*, 2007, **46**, 5791–5797.
- 311 O. Krocher, R. A. Koppel, M. Froba and A. Baiker, *J. Catal.*, 1998, **178**, 284–298.
- 312 O. Krocher, R. A. Koppel and A. Baiker, *J. Mol. Catal. A: Chem.*, 1999, **140**, 185–193.
- 313 Y. Kayaki, Y. Shimokawatoko and T. Ikariya, *Adv. Synth. Catal.*, 2003, **345**, 175–179.
- 314 L. Schmid, A. Canonica and A. Baiker, *Appl. Catal., A*, 2003, **255**, 23–33.
- 315 L. Schmid, M. S. Schneider, D. Engel and A. Baiker, *Catal. Lett.*, 2003, **88**, 105–113.
- 316 P. Munshi, D. J. Heldebrant, E. P. McKoon, P. A. Kelly, C. C. Tai and P. G. Jessop, *Tetrahedron Lett.*, 2003, **44**, 2725–2727.
- 317 M. Rohr, J. D. Grunwaldt and A. Baiker, *J. Mol. Catal. A: Chem.*, 2005, **226**, 253–257.
- 318 M. Rohr, J. D. Grunwaldt and A. Baiker, *J. Catal.*, 2005, **229**, 144–153.
- 319 O. S. Joo, K. D. Jung, S. H. Han, S. J. Uhm, D. K. Lee and S. K. Ihm, *Appl. Catal., A*, 1996, **135**, 273–286.